Environmental Science & Technology
2022, Volume 56, Issue 7, Pages 3840-3862
https://doi.org/10.1021/acs.est.1c03044
https://archimer.ifremer.fr/doc/00754/86597/

Mediterranean Mercury Assessment 2022: An Updated Budget, Health Consequences, and Research Perspectives

Cossa Daniel [1, *], Knoery Joel [2], Bănaru Daniela [3], Harmelin-Vivien Mireille [3], Sonke Jeroen E. [4], Hedgecock Ian M. [5], Bravo Andrea G. [6], Rosati Ginevra [7], Canu Donata [7], Horvat Milena [8], Sprovieri Francesca [5], Pirrone Nicola [5], Heimbürger-Boavida Lars-Eric [3]

[1] Université Grenoble Alpes, ISTerre, CS 40700, 38058 Grenoble Cedex 9, France
[2] Ifremer, Centre Atlantique de Nantes, BP 44311, 44980 Nantes, France
[3] Aix Marseille Université, CNRS/INSU, Université de Toulon, IRD, Mediterranean Institute of Oceanography (MIO) UM 110, 13288 Marseille, France
[4] Géosciences Environnement Toulouse, CNRS/Observatoire Midi-Pyrénées (OMP)/Université de Toulouse, 31400 Toulouse, France
[5] Istituto sull'inquinamento atmosferico, CNR-IIA, 87036 Rende, Italy
[6] Institut de Ciències del Mar, 08003 Barcelona, Spain
[7] Istituto Nazionale di Oceanografia e di Geofisca Sperimentale (OGS), 34010 Trieste, Italy
[8] Institut Józef Stefan, 1000 Ljubljana, Slovenija

* Corresponding author : Daniel Cossa, email address : dcossa@ifremer.fr

Abstract :

Mercury (Hg) and especially its methylated species (MeHg) are toxic chemicals that contaminate humans via the consumption of seafood. The most recent UNEP Global Mercury Assessment stressed that Mediterranean populations have higher Hg levels than people elsewhere in Europe. The present Critical Review updates current knowledge on the sources, biogeochemical cycling, and mass balance of Hg in the Mediterranean and identifies perspectives for future research especially in the context of global change. Concentrations of Hg in the Western Mediterranean average 0.86 ± 0.27 pmol L–1 in the upper water layer and 1.02 ± 0.12 pmol L–1 in intermediate and deep waters. In the Eastern Mediterranean, Hg measurements are in the same range but are too few to determine any consistent oceanographical pattern. The Mediterranean waters have a high methylation capacity, with MeHg representing up to 86% of the total Hg, and constitute a source of MeHg for the adjacent North Atlantic Ocean. The highest MeHg concentrations are associated with low oxygen water masses, suggesting a microbiological control on Hg methylation, consistent with the identification of hgcA-like genes in Mediterranean waters. MeHg concentrations are twice as high in the waters of the Western Basin compared to the ultra-oligotrophic Eastern Basin waters. This difference appears to be transferred through the food webs and the Hg content in predators to be ultimately controlled by MeHg concentrations of the waters of their foraging zones. Many Mediterranean top-predatory fish still exceed European Union regulatory Hg thresholds. This emphasizes the necessity of monitoring the exposure of Mediterranean populations, to formulate adequate mitigation strategies and recommendations, without advising against seafood consumption. This review also points out other insufficiencies of knowledge of Hg cycling in the Mediterranean Sea, including temporal variations in air–sea exchange, hydrothermal and cold seep inputs, point sources, submarine groundwater discharge, and exchanges between margins and the open sea. Future

assessment of global change impacts under the Minamata Convention Hg policy requires long-term observations and dedicated high-resolution Earth System Models for the Mediterranean region.

Graphical abstract

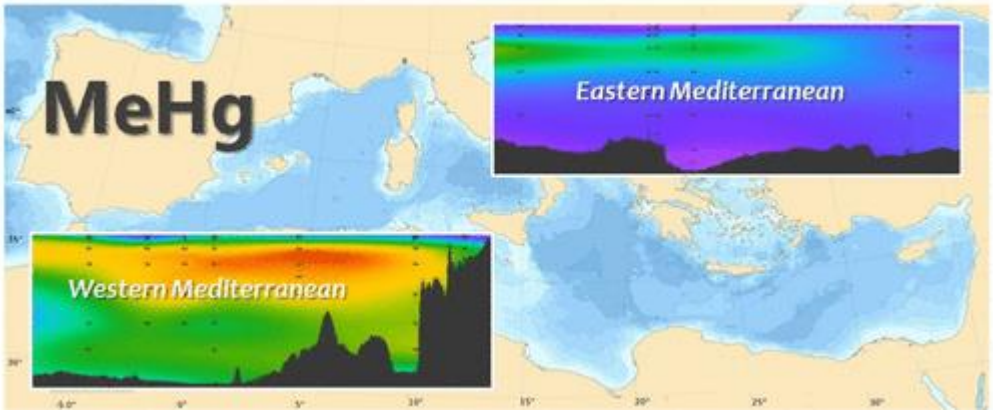

Keywords : Mediterranean, Mercury, Hg, MeHg, Earth System Models

Introduction

Mercury (Hg) has been classified by the United Nations Environment Programme (UNEP) as a chemical element toxic to living organisms including humans[1, 2, 3]. One group of its compounds, methylated mercury (MeHg), damages the human nervous system[4, 5, 6], and has been linked to cardiovascular disease[7]. Exposure of top predators to MeHg is caused by its high biomagnification potential within aquatic food webs[2, 8,]. Marine fish consumption is the main source of MeHg to humans[2, 8, 9, 10]. Hg is of global environmental concern, because of the major perturbation of its natural cycle by human activities, its long-distance transport *via* the atmosphere resulting in its ubiquity in terrestrial and marine ecosystems, and finally because of its long persistence in biologically-crucial zones of the aquatic environment[11, 12, 13]. The global issue of Hg has begun to be confronted by the adoption of the Minamata Convention, which entered into force in 2017 under the auspices of UNEP to reduce human and ecosystem Hg exposure.

The recent Global Mercury Assessment (GMA 2018)[1] highlighted key policy-relevant findings and includes an updated inventory of anthropogenic Hg releases: artisanal and small-scale gold mining, fossil fuel and biomass burning, waste incineration, smelters, and from the re-mobilization of anthropogenic Hg deposited in the past to soils, sediments, water bodies, dumping grounds, and mine-tailings. Anthropogenic Hg emissions have been substantial since the Industrial Era, and have left a detectable environmental imprint for more than 2000 years[14]. Moreover, it has been estimated that 95% of Hg emissions occurred in the last 500 years and that they have increased by 1.8% per year during the 2010-2015 period[15, 16]. The global Hg budget, updated in 2018[13], states that current Hg concentrations in the global atmosphere, surface, and deep marine waters have increased respectively by 450, 230, and 12-25% above levels prevailing during the pre-Colombian period[11], i.e., before ~1450 CE. This budget however presents large uncertainties, in particular, local differences are to be expected, due to specific geographical, geological, biological, and anthropogenic factors.

The GMA 2018[1] also stresses that Mediterranean (MED) populations tend to have higher Hg levels than people from Asia, North America, and Europe. Already, 50 years ago, high Hg levels were observed in MED fish and marine mammals[17, 18], and these findings have been confirmed several times[19, 20, 21]. It has been recently suggested that Hg accumulation rates in bluefin tuna are the highest in the individuals from the MED[22] and that certain birds linked to the marine ecosystem could be at risk of suffering long-term, Hg-related effects[23]. These observations suggest specific features and a particular vulnerability of this region and emphasize the need to reassess, there, the state of the art on Hg. The present Critical Review aims to summarize and update current knowledge on the biogeochemistry of Hg in the MED, including its main implications for human health, and to identify perspectives for future research activities in this field.

1. The marine mercury cycle and relevant Mediterranean-specific features

The main chemical reactions within the Hg cycle in the environment may be roughly summarized by the interconversions of elemental Hg (Hg^0), inorganic divalent Hg (Hg_i^{II}), and organic divalent, including mono- and dimethylated species (CH_3Hg^+/MMHg and CH_3HgCH_3/DMHg, hereafter collectively abbreviated as MeHg). Mobility through the atmosphere is favored by volatile Hg^0, and through the hydrosphere by the solubilities of

various Hg^{II} species. A summary of the latest scientific advances on the global Hg biogeochemical cycle is available in a recent paper[24]. Due to its volatility, Hg is dispersed in the global atmosphere. Part of it is redeposited onto continental and sea surfaces, where it is incorporated into biota mainly as MeHg. MeHg biomagnification along the food web is the main source of Hg for top predators, with a bioconcentration factor[25] up to 10^7. The result is that some marine predators eaten by human populations or other animals are the main sources of their exposure to MeHg and as such a major risk of Hg poisoning[8]. A more detailed summary of the biogeochemical Hg cycle is given in the Supporting Information (SI.1).

The MED is a semi-enclosed sea (Fig. 1), with a water residence time of around 100 years, characterized by marked North-South and East-West gradients, mainly driven by the different physiographies of the two basins, the different terrestrial nutrient loadings, and the cyclonic and anticyclonic wind-driven current structures[26, 27]. The geological context, the contrasting hydrodynamic regimes, and the biogeochemical functioning of the MED have several characteristics important to the MED Hg cycle. In addition, the MED has been identified as a climate change hotspot[28, 29].

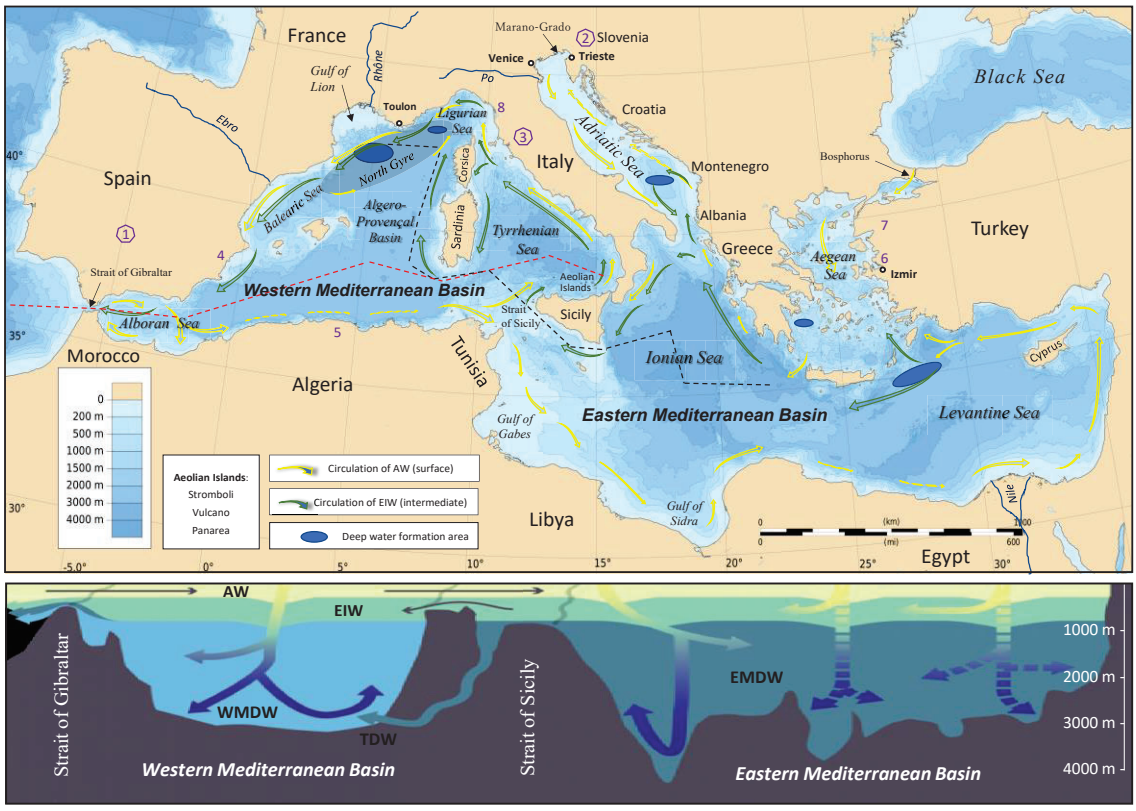

***Figure 1**. The Mediterranean Sea with its main rivers and a schematic of water circulation. Purple numbers refer to Hg ore deposits: (1) Almaden, Spain, (2) Idrija, Slovenia, and (3) Monte Amiata are the main ones; other minor Hg deposits include (4) Azogue Valley (Pulpi), Spain, (5) Numidia, Algeria, (6) Karaburn, Turkey, (7) Kuçukyenice, Turkey, and (8) Levigliani, Italy. The red dash line refers to the Figure 2 transect. The black dash line refers to the Figure 3 transect. Dash arrows refer to seasonal circulation paths. The lower part of the figure is modified from Ref. 27. www.ifremer.fr/lobtln/COURANTS/SCHEMA_3D_MED_LABELS_EN.jpg.*

The Iberian Hg belt, where cinnabar (HgS) is the principal Hg ore, is found along the edges of the MED. It extends from Spain (Almaden) to Italy (Monte Amiata), Slovenia (Idrija), Algeria (Numidia belt), and Aegean Turkey (Karaburun) (Fig. 1). In addition to these natural sources, mining and other anthropogenic activities have mobilized large quantities of Hg that are now buried in coastal sediments. Among the most relevant anthropogenic legacy Hg hotspots in the MED, are the Gulf of Trieste (with 13 000 Mg of anthropogenic Hg accumulated in the sediments[30, 31]), Marano Grado Lagoon (271 Mg[32]), Venice Lagoon (20 Mg[33]) in the Eastern MED (EMED), and the Toulon Bay (26 Mg[34]) in the Western MED (WMED) (Fig. 1). These Hg reservoirs can maintain steady inputs to the water column. Also, Hg-laden sediments may be remobilized and transported off-shore during floods or storms. Mercury inputs to the MED from hydrothermal vents are suspected but are not yet constrained[35]. Elevated Hg concentrations have been found in shallow hydrothermal fluids[36] and terrestrial volcanoes[37]. Subaerial volcanic Hg emissions in the Mediterranean region are dominated by the Aeolian Island volcanoes Vulcano and Stromboli, and by Mt Etna in Sicily[38] (Fig. 1).

Since it has become possible to determine accurately ultra-trace levels of Hg in ocean waters, several mass budgets for Hg in the MED have been established[39, 40, 41]. The first budget concludes that Hg entered through the Gibraltar Strait as inorganic Hg and was exported to the North Atlantic Ocean with a larger proportion of MeHg[39]. Another conclusion was that atmospheric exchanges are the main source and sink of Hg in the MED[41]. Hg exchanges at the sediment/water interface and the influence of hydrothermal vents are currently much less well constrained. The ultimate sources of water-column MeHg are currently under debate[42, 43]. The experimental estimates of Hg methylation rates[44, 45] suggest that the consequence of even a small change in these transformation rates would have a major impact on the levels of MeHg, which is the main factor governing the entry of Hg into the food webs. Continental Hg sources, namely rivers and groundwaters, have not yet been considered with sufficient attention in the karstic MED environment. Large discrepancies also exist between estimates of Hg

transport in water masses, due to variations in Hg water column concentrations over the last 30 years[39, 40, 41]. These variations in Hg flux estimates may be due to (i) the observed decrease in Hg concentrations in North-Atlantic surface waters which can be over 50% between 1989 and 2012[46], but also to (ii) variations in the surface water inflow estimated at Gibraltar[47]. Furthermore, the residence time of water in the WMED is shorter than 50 years and biogeochemical conditions and Hg fluxes may vary over a decadal time scale[27, 29]. In summary, the steady-state Hg fluxes in the different MED biogeochemical compartments are far from being well-established, warranting a revisit of Mediterranean Hg dynamics and budget. Moreover, Hg accumulation in biota is a multi-causal process[21, 48] that is ultimately determined not only by past Hg emissions and their temporal evolution, but also by changes in biogeochemical, climate-induced, and biologically mediated processes[49]. Thus, the ecological and health consequences of the present Hg cycle in the MED will likely further evolve with the climate changes expected over the next decades.

2. Updating the Mediterranean Hg cycle

2.1. Emissions, evasions, and deposition

An early assessment of the total anthropogenic Hg emissions of countries bordering the MED was about 100 Mg for the year 1995 (i.e., equivalent to a third of European or 5% of global anthropogenic emissions)[50]. Thirty (30) Mg resulted from the burning of fossil fuels, 29 Mg from the incineration of household wastes, 28 Mg from cement production, and 10 Mg from the production of chlorine and lye. In addition, the total amount of Hg released to the atmosphere from forest fires in the Mediterranean region[51] accounted for 4.3 Mg y^{-1} and 7 Mg y^{-1} from volcanoes (see section 2.5.). The GMA 2018[1] indicates that between 2010 and 2015 anthropogenic emissions from the (then) EU28 (EU28 was the abbreviation of the 28 countries of the European Union) decreased by 12.5% while those from North Africa increased slightly (+15.8%). Both EU28 and North Africa increased in large-scale gold production, and while the EU28 countries reduced emissions from the oil industry and power plants, North Africa increased emissions from domestic and industrial fossil fuel combustions. The phasing out of Hg in chlor-alkali plants in EU28 led to a two-thirds reduction in emissions from chemical industries.

Since the year 2000, numerous oceanographic and more local near-coast measurement campaigns have been carried out to determine Hg species concentrations in the marine boundary layer and the water column[52, 53, 54, 55, 56]. Evasion fluxes of Hg are calculated using measured dissolved gaseous mercury (DGM) and $Hg^0_{(g)}$ concentrations, wind speed, and sea surface temperature, and several approaches can and have been used to estimate MED efflux/volatilization/atmospheric rates[57, 58, 59, 60]. Details about the modeling approaches to calculate gas transfer velocities at the air-sea interface are given in Supporting Information (SI.2)[61, 62, 63, 64, 65, 66, 67, 68, 69, 70, 71].

Averaged Hg evasion fluxes for the MED are reasonably consistent across the literature, 2-8 ng m^{-2} h^{-1}, with higher values typically found in summer and autumn (up to 20 ng m^{-2} h^{-1} was reported[60] for a short period), and for the Eastern Basin compared to the Western Basin[57, 58, 59, 60]. The higher values obtained for the Eastern Basin stem possibly from tectonic activity. These fluxes lead to estimates of annual evasion of Hg^0 to the atmosphere between 50 and 100 Mg y^{-1} (Table 4 in Ref. 71). While the estimated average fluxes are close between the studies, all the above studies indicate that the Hg^0 flux to the atmosphere can be extremely variable over space and time. Indeed, they depend on DGM concentrations, temperature, and exponentially on wind speed, which are all highly variable. There are also several Hg "hot spots" in the MED, both due to tectonic activity and regions impacted by anthropogenic activities where significantly higher evasion fluxes can occur[72, 73]. A description of atmosphere surface exchange measurement techniques can be found in a recent review[74].

Mercury deposition to the MED is a combination of Hg^{II} wet deposition (rainfall), dry deposition of gaseous, and particulate oxidized Hg^{II} forms. There are several "European Monitoring and Evaluation Programme" sites that measure Hg wet and/or dry depositions. Unfortunately, only 3 of these are in or near the MED basin, and measure wet deposition only: Iskrba, Slovenia, at 500 m a.s.l., Longobucco, in Southern Italy, at 1358 m a.s.l., and Ostriconi, in Corsica, at 100 m a.s.l. Annual Hg wet deposition at these sites is 6.7, 1.7, and 3.0 μg m^{-2} y^{-1} respectively[75, 76]. The paucity of representative measurement data for the MED is an issue that needs to be addressed. Hg deposition to the MED has therefore been estimated from knowledge of the concentration of Hg^0 and its oxidants in the region, the rate of atmospheric oxidation processes which lead to the formation of Hg^{II}, and wet and dry deposition processes. Gencarelli et al.[77] used a version of WRF-Chem to estimate dry and wet deposition

fluxes to the MED. They found that the modeled contributions to deposition were almost equal, 19.6 and 18.1 Mg y^{-1} dry and wet, respectively. No observational data exist for Hg dry deposition. Combined with modeled annual evasion of Hg^0 from the sea surface of 67.5 Mg y^{-1} (in agreement with most of the estimates from the studies above), the model budget gives a net annual evasion flux of 30 Mg. A further model study showed that dry deposition accounted for more than half the Hg deposited to the MED in the summer months, and between 40 and 50% of the annual total deposition, depending on the atmospheric Hg oxidation mechanism employed in the model[78]. Synoptic scale wet deposition of Hg contributes roughly ten times more to the total Hg deposition than convective wet deposition and is the dominant source of Hg to the MED from Autumn through to Spring. Most Hg deposition to the MED is due to transport from distant sources, except in the summer when sources from countries surrounding the MED have a greater influence due to the prevailing meteorological conditions. This is reflected in the change in the total modeled deposition to the MED when using anthropogenic emission databases for 2005 and 2010, where a 33% reduction of in-domain emissions resulted in a 12% deposition decrease. A global modeling study[79] suggested that slightly more than 20% of Hg deposited to the MED comes from primary anthropogenic sources. A recent study[80] estimates that a 50% reduction in EU emissions, would only lead to a 17% decrease in Hg deposition to the MED.

The recent advances in understanding the processes driving atmospheric Hg redox chemistry[81, 82, 83, 84], and also in coupling ocean and atmosphere models[69, 71], suggest that it would be an appropriate time for high-resolution MED modeling studies to be conducted again. Potentially the photolytic reduction of Hg^{II} compounds in the atmosphere[82] could have a significant role in the cycling of Hg between the atmosphere and seas. Gas-phase reduction of Hg^{II} could decrease model estimates of both Hg^{II} wet and dry deposition to the MED, by a proportion that needs yet to be modeled. Given the dominance of Hg long-range transport and the synoptic rain fluxes, the chemical reduction of gaseous Hg^{II} likely has a small impact. Gas-phase reduction of Hg^{II} could decrease model estimates of both Hg^{II} wet and dry deposition to the MED, by a proportion that needs yet to be modeled, and that is supported by recent Hg stable isotope observations of Hg in the MED[85].

Despite the questions remaining regarding the exact nature of atmospheric Hg redox pathways, there is little doubt that the MED is a net source of Hg to the atmosphere,

with roughly 60-80 Mg y^{-1} is emitted to the atmosphere while it is estimated that dry and wet deposition amount at around 20 Mg y^{-1} each.

2.2. The waters of the Mediterranean Sea

2.2.1. Geographical distribution of total mercury (THg)

The vertical structure of the WMED water column can be schematically subdivided into three major water masses: (i) Atlantic Water (AW), (ii) Eastern Intermediate Water (EIW), and (iii) Western Mediterranean Deep Water (WMDW)[27] (Fig. 1). AW (from the surface to ~ 250 m) is a low salinity water mass entering the MED at Gibraltar, and spreading eastward into the entire basin. EIW is a high salinity water mass, located just below AW and down to ~600 m, originating in the EMED. Below that depth and down to the seabed is the WMDW formed in the WMED during winter convection periods, which fills the entire basin. In addition, in the Tyrrhenian basin, Tyrrhenian Deep Water (TDW) is formed as the result of the deep mixing of waters from eastern and western MED (Fig. 1).

Figure 2 illustrates a recently measured distribution of THg across the western basin (WMED). Summarized statistics of THg concentrations (pmol L^{-1}) in the WMED waters measured between 2000 and 2017 are given in the Supporting Information (SI.3). In open waters, the <0.45 µm fraction represents 89% of the THg in waters. High and low THg concentrations are present in the AW (0.21-2.01 pmol L^{-1}) averaging 0.86 ± 0.27 pmol L^{-1}. Within the EIW and WMDW, the concentrations vary over a narrower range (0.51-1.62 pmol L^{-1}) averaging 1.02 ± 0.12 pmol L^{-1}. The highly variable concentrations in AW are the consequence of air-sea exchange dynamics which govern the balance between Hg deposition and evasion from the sea surface, and primary production, which governs the downward Hg biological pump. In places where deep convection occurs (i.e., the Ligurian Sea and the Gulf of Lion), transferring the surface layer and its Hg level to depth, a local Hg-enrichment (or depletion) of the WMDW can be observed compared to the rest of the Western Basin. By comparison, the THg concentrations in the waters of the WMED margins (Gulf of Lion) are slightly higher: 1.52 ± 1.00 pmol L^{-1} in the inner shelf, 1.09 ± 0.15 pmol L^{-1} along the slope, and 1.10 ± 0.13 pmol L^{-1} in the Northern Gyre. These higher concentrations result from the higher particulate Hg load of shelf waters[86] rather than dissolved Hg species. In the open waters of the eastern basin (EMED) Hg measurements are scarce. The first "oceanographically consistent" profile showed little vertical THg variation (mean = 1.01 ± 0.08 pmol L^{-1}, n = 22)[75]. Note that

"oceanographic consistency" means, among other criteria, that vertical profiles should be smooth and relatable to established oceanographic features[87]. In contrast, more data are available from the Adriatic Sea. This region, consisting of a large continental shelf, exhibits high THg concentrations and strong geographical gradients due to Hg mining and industrial sources[88].

No temporal trend has been detected in the THg concentrations listed in the Supporting Information (SI.3). However, a significant decrease in concentration in the Alboran Sea and the adjacent Northeast Atlantic waters was observed over a 20-year period[46]. Based on the results of THg in water columns on both sides of the Strait of Gibraltar between 1989 and 2012, it was proposed that a 30% decrease of THg has occurred in the deep layer which flows out of the MED, whereas a50% decrease has occurred in the Atlantic waters entering the MED.

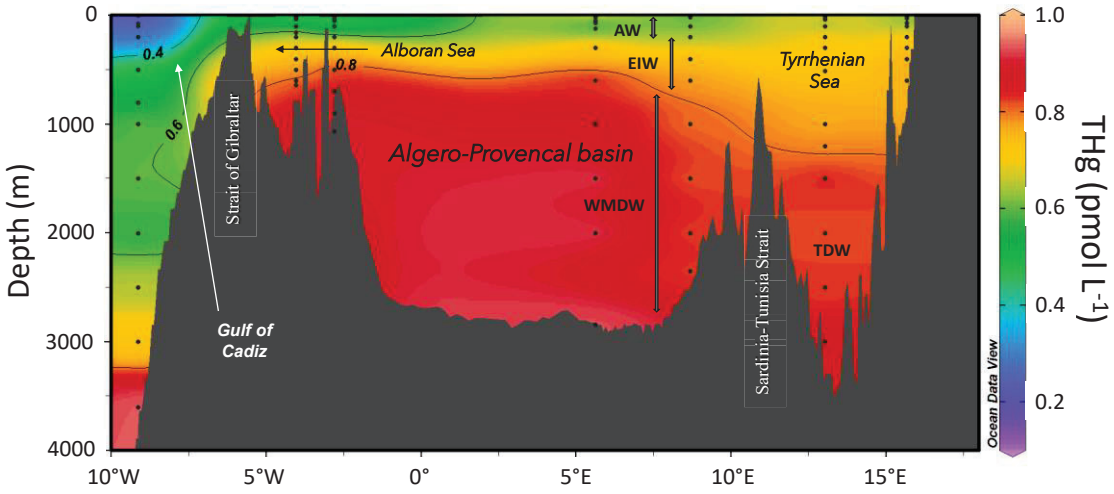

Figure 2. *Distribution of total Hg in unfiltered samples (THg) distribution across the WMED during* FENICE *cruise (2012). AW: Atlantic Water, EIW: Eastern Intermediate Water, WMDW: Western Mediterranean Deep Water, TDW: Tyrrhenian Deep Water. The path of the transect is the red dash line in Figure 1.*

296 *2.2.2. Geographical distribution of methylated mercury (MeHg)*

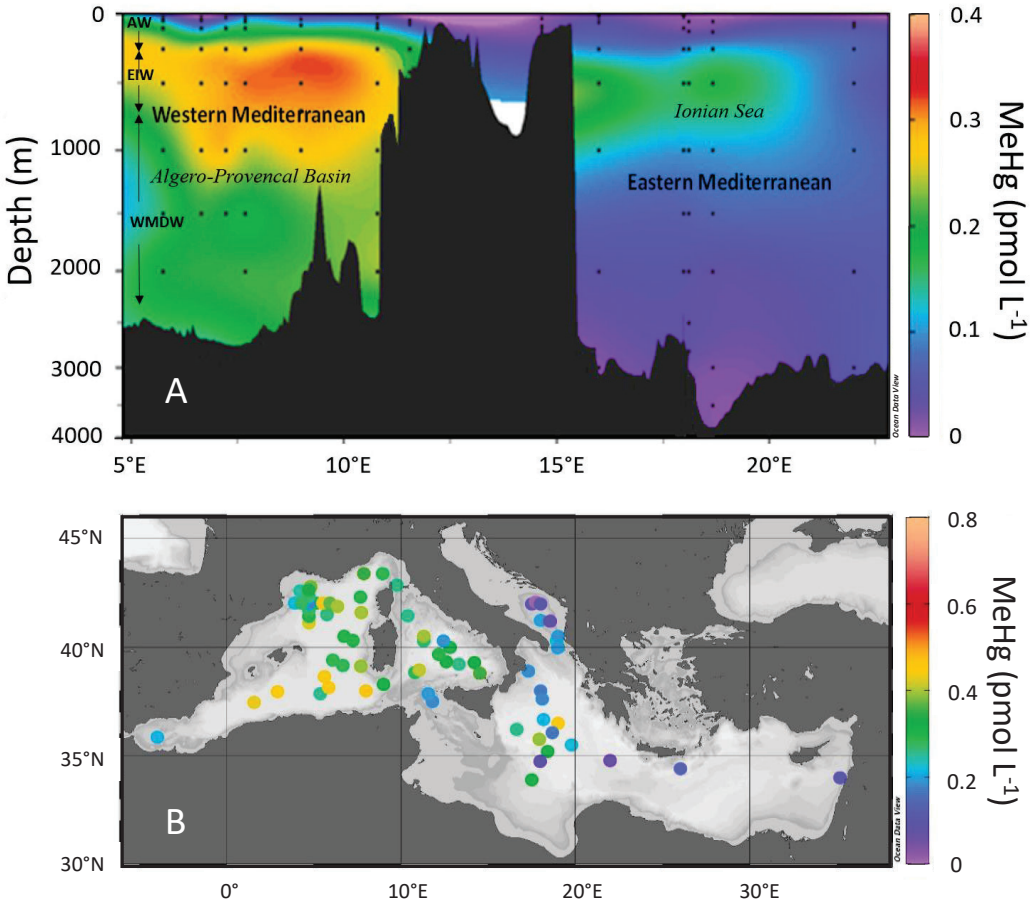

297

298 ***Figure 3.*** *Panel A: Methylated Hg (MeHg) in unfiltered samples during ALDEBARAN cruise*
299 *(2009). AW: Atlantic Water, EIW: Eastern Intermediate Water, WMDW: Western*
300 *Mediterranean Deep Water, TDW: Tyrrhenian Deep Water. The path of the transect is the black*
301 *dash line in Figure 1. Panel B: MeHg in unfiltered samples from 400 m during MEDSHIP cruise*
302 *(2011).*

303

304 Recent MeHg measurements[89, 90] display concentration ranges from <0.02 pmol L^{-1}
305 up to 0.71 and up to 0.23 pmol L^{-1} for the WMED and EMED waters, respectively. The
306 MeHg:THg ratios vary from 0.01 to 0.86. The highest values are found in the oxygen
307 minimum zones (OMZ). These ranges are similar to other ocean basins (Supporting
308 Information, SI.4). MeHg concentrations vary spatially (Fig. 3) with higher levels in the
309 WMED compared to the EMED, and over-time as shown by time-series in the Ligurian
310 Sea (WMED)[91]. MeHg was positively correlated with oxygen consumption (Fig. 4),
311 especially within aphotic layers, namely EIW and DMW ($MeHg_{pM}$ = 0.004 $AOU_{\mu M}$ –
312 0.017 (R^2 = 0.58, n = 301, p< 0.001). Regression coefficients (molar ratios) of MeHg *vs*

apparent oxygen utilization (AOU) relationships, assumed to be a proxy for the Hg methylation capacity of a water mass, varied between 2.1 x 10^{-3} and 6.6 x 10^{-3} during a number of Mediterranean cruises. Compared with values obtained in the North, Equatorial, South Pacific[92, 93], the Southern Ocean[94], and the North Atlantic[95], the methylation capacity of intermediate waters of the MED is the highest. Methylation in the OMZ results from microbiological activity in association with OM regeneration[92, 96, 97, 98]. Low MeHg concentrations were found in waters overlying the continental shelves of the Northern Adriatic and Gulf of Lion[43, 88].

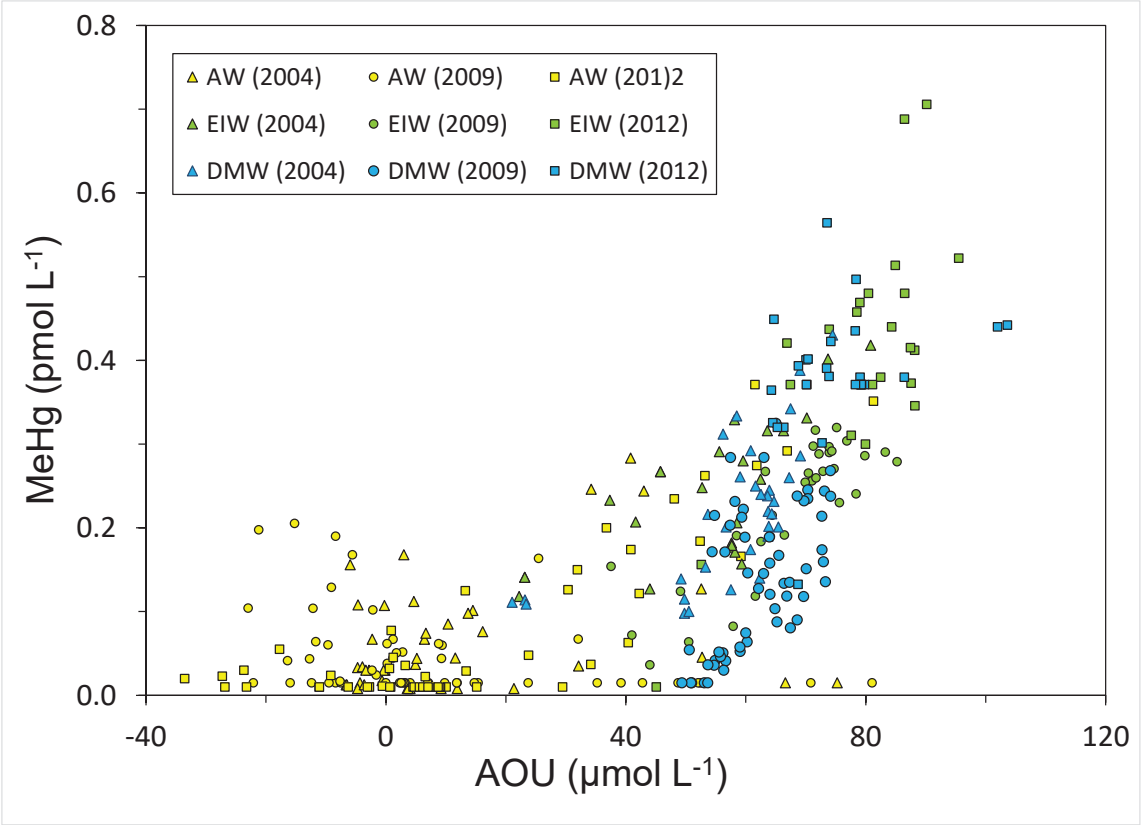

Figure 4. *Methylated Hg (MeHg)* vs. *Apparent Oxygen Utilization (AOU) during MEDOCEANOR-3 (April 2004), ALDEBARAN (June 2009), and FENICE cruises (August 2012). Colors refer to various water masses (yellow for AW, green for EIW, and blue for DMW, Fig. 1). The shapes of symbols refer to the different cruises.*

Mono- and dimethylmercury have been identified in Mediterranean waters[39, 43, 99]. However, observed MMHg:DMHg ratios vary inexplicably in space and time. This possibly indicates a very fast interconversion of the two Hg methylated species or more likely analytical difficulties. Thus, the first step to address this issue would be to acquire additional quality-controlled data on Hg speciation. The second step would be to further

explore the mechanisms for Hg_i^{II} methylation in oxic oceanic waters. Suboxic/anoxic microzones of the marine snow may be suitable environments for microbiological Hg methylation, as has been suggested for settling particles in lakes[100]. In marine oligotrophic waters, such as those of the EMED, findings suggest an important role for a noncellular or extracellular methylation mechanism[101].

2.2.3. Dissolved gaseous Hg

Generally, DGM represents 1/5th of the THg in Mediterranean waters and it would consist, mostly of dissolved Hg^0 if DMHg data are correct. Vertical profiles of DGM presents large spatial and temporal variations from a few tenths to 1.4 pmol L^{-1}, with high concentrations found in intermediate and deep waters (e.g., EIW, WMDW, and EMDW) compared to AW[88], and frequent increases in the hypoxic layer. This is coherent with a microbially-mediated Hg reduction to DGM species. Finally, a possible geotectonic origin for DGM exists in the hydrothermal zones of the MED[102]. In coastal areas of the Adriatic Sea, the influence of anthropogenic Hg on DGM has been suggested[88].

2.3. The sediments of the Mediterranean Sea

Sediment cores were collected on the abyssal plain of the MED[42, 75, 103]. Some THg vertical profiles in sediment cores from the abyssal plain of the MED are shown in Figure 5. The use of Hg stable isotopes allowed us to suggest anthropogenic sources for Hg in Mediterranean surface sediments[104]. A recent paper[105] shows that Hg accumulation rates rose from 0.4 to 8.6 µg m^{-2} y^{-1} in the last 6000 years, with a maximum deposition in the last 120 years. According to the same authors, the accumulation rate for the year 2001-2002 measured with a sediment trap, located 20 m above abyssal sediments, was 3.1 ± 0.5 µg m^{-2} y^{-1} and suggests to Hg fluxes to the deep WMED sediments of 4.2 Mg y^{-1}. The rare MeHg determinations in open MED sediments indicate that it would represent between 0.5 to 2% of the THg[42, 106]. A MeHg diffusive flux from deep sediments to the water column was estimated[42] between 0.2 and 2.3 µg m^{-2} y^{-1}, which represents more than 50% of the deposition; these are probably largely overrated. For the EMED deep sediments, we based our calculation on a sedimentation rate ratio of 0.68 between EMED and WMED[107] and a Hg concentration in EMED surface sediment of half of the WMED (Fig. 5). With these assumptions, the Hg accumulated each year in the deep sediment of the EMED is ~1.6 Mg. Mercury accumulation on MED coastal sediments is more documented particularly on the shelves

of the Gulf of Lion (WMED)[86] and of the Adriatic Sea (EMED)[88, 108] where Hg hotspots were identified. Extrapolating these data, the Hg accumulated each year on the shelf is 3.6 and 3.2 Mg for Western and Eastern basin shelf sediments, respectively. However, the shelf sediments may not be a permanent sink, and turbiditic currents and cascading phenomena may export part of the sediment to the abyssal plain trough canyons[109].

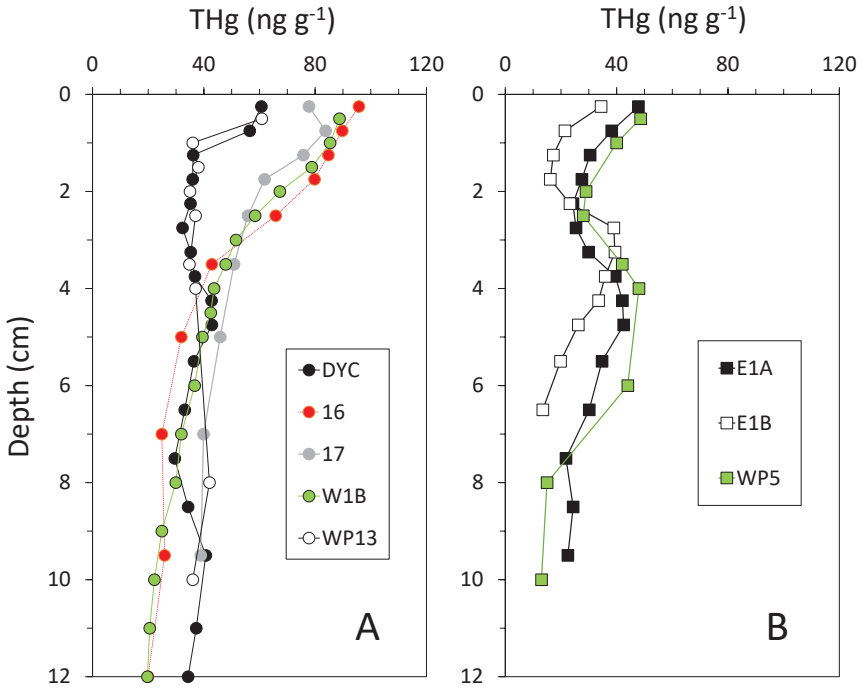

***Figure 5**. Total Hg concentration (THg) profiles in sediment cores from the abyssal plain (bottom > 2000m) of the Western Mediterranean (A) and Eastern Mediterranean (B). (DYC) Ligurian Sea[103]; (WP13, WIB, 16 and 17) Algero-Provençal basin[42, 75]; (E1A and E1B) Ionian Sea[75]; (WP5) Levantine Sea[42].*

2.4. Exchanges with the Atlantic Ocean

Using water mass fluxes and updated THg concentrations from Table 1, the Hg inflow entering the MED at the Strait of Gibraltar is 2.54 ± 0.26 Mg y^{-1}. This estimation is more than 3 times lower than the 7.5 Mg y^{-1} estimated in the previous budget[41]. On the other hand, Hg outflow to the North Atlantic Ocean is 3.99 ± 0.76 Mg y^{-1}, a value also smaller than the preceding estimate (6.5 Mg y^{-1})[41]. The largest difference of this budget compared to the previous transport calculation at the Gibraltar Strait is the net export of "Mediterranean Hg" to the adjacent North Atlantic Ocean of ~1.9 Mg y^{-1}. This export is consistent with the Hg-enriched Mediterranean water lenses found at the salinity maximum in the North-East Atlantic Ocean water column[110]. Thus, the MED is a source

of Hg for the adjacent Eastern North Atlantic Ocean, as it is also for lead[111], another anthropogenic trace metal still abundant in the MED. Considering the MeHg fluxes, the excess of Mediterranean export to the Atlantic is more marked, since MeHg is maximum at depth (with outflowing waters at Strait of Gibraltar) and demethylation of MeHg occurs in inflowing surface waters. Using the water fluxes at Gibraltar of 0.85 Sv and the MeHg concentrations of 0.25 pmol L^{-1}, this export of Mediterranean MeHg to the North Atlantic Ocean is 1.35 Mg y^{-1}.

Table 1. *Average concentrations (± standard deviation) of total Hg (THg) and methylated Hg (MeHg) and derived fluxes at the Strait of Gibraltar. 1 Sv = 10^6 m^3 s^{-1}. (*) at Espartel sill according to Ref. 112. THg concentrations from Ref. 46. MeHg concentrations from Ref. 90.*

Water mass	Water flux* (Sv)	THg (pmol L^{-1})	Hg flux (kmol y^{-1})	MeHg (pmol L^{-1})	MeHg flux (kmol y^{-1})
Atlantic inflow	0.89 ± 0.12	0.45 ± 0.05	12.6 ± 2.3	<0.05	<1.4
Mediterranean outflow	0.85 ± 0.13	0.83 ± 0.13	22.3 ± 3.8	0.26 ± 0.09	6.9 ± 1.2

2.5. Volcanic and hydrothermal emissions

Subaerial volcanic Hg emissions in the Mediterranean region are dominated by the Aeolian volcanoes Vulcano and Stromboli, and by Mt Etna in Sicily. A cruise campaign to the south-western sector of the Mediterranean Basin during summer 2015 studied the potential impact of continuously active volcanoes of the Aeolian arc on observed atmospheric Hg concentrations[113]. Increases in GOM (Gaseous Oxidized Mercury) concentrations, often during night time (30 pg m^{-3} with peaks of 129 pg m^{-3}), were observed close to Stromboli volcano in the air originating from it, simultaneously with an increase in both SO_2 and GEM (Gaseous Elemental Mercury). There are currently many difficulties in quantifying the Hg flux from volcanic emissions due to the spatial and temporal variabilities in the activity from one volcano to another[37, 114], or from different emission sites on the volcano[115].

Ferrara et al.[37] measured Hg/SO_2 ratios at Vulcano and used these to calculate passive Hg emissions ranges for Vulcano (1.3 – 5.5 kg y^{-1}), Stromboli (7.3 – 77 kg y^{-1}), and Etna (0.06 – 0.54 Mg y^{-1}) by multiplying with field-based SO_2 emission estimates. Here we use a mean global volcanic Hg/SO_2 ratio of $7.8 \pm 1.5 \times 10^{-6}$ (n = 13, Ref. 116) and modern satellite-based SO_2 emissions for Stromboli and Etna[117] between 2005-2015 to estimate passive degassing Hg emissions of 0.5 ± 0.3 Mg y^{-1} for Stromboli and 5.8 ±

1.8 Mg y^{-1} for Etna. Remote sensing SO_2 data is not available for Vulcano, so we cannot refine its budget here. Global eruptive volcanic SO_2 emissions, estimated by remote sensing, are indicated to be one order of magnitude smaller (8.8x) than passive degassing[117]. We, therefore, estimate the sum of passive and eruptive aerial volcanic Hg emissions in the MED region to be 7.0 ± 2.3 Mg y^{-1}.

Two recent GEOTRACES cruises found elevated Hg levels crossing the Mid Atlantic Ridge and no distinct Hg signal crossing the East Pacific Rise in the vent plumes[118, 119]. The results and implications are either contradictory or point to strong site-specificity and temporal dynamics. Some contradictory data exists for hydrothermal systems in the deep ocean[35], but no deep vents exist in the MED. Hydrothermal systems in shallow (less than 200 m-depth), near-shore environments have been largely ignored, and their contribution to the global Hg cycle remains unknown[13]. In the MED several shallow sites are known (e.g., Milos). A first investigation of the Panarea site (Italy)[36] shows significant Hg inputs, especially Hg^0. The study finds that the Hg^0 evasion flux is negligible in the MED budget. The authors state that previous assessments[40, 41] of total hydrothermal inputs to the MED ~15 Mg y^{-1}, are underestimations. This possibly important source is far from being well-constrained; obviously, more data are crucially needed in this field.

2.6. Riverine and submarine groundwater discharge

According to a recent paper[120], riverine discharge from European rivers into the MED is 2.9 Mg y^{-1}; this input is highly seasonal due to the Mediterranean hydrological regime[75]. However, the inputs from rivers into the eastern and southern parts of the MED shore are not included in this inventory. The way we have chosen to assess the total Hg riverine influxes to the MED is by extrapolating the mean Hg concentrations (2.45 pmol L^{-1}, 0.85 nmol g^{-1}, for dissolved and particulate Hg, respectively) of the Rhône River, for which multi-year time-series exist[43], to the total MED river discharge. We arrive at a total Hg input of 6 Mg y^{-1}, which is divided into 2.3 and 3.7 Mg y^{-1} for the Western and Eastern basins, respectively. Hydrological data used for these calculations are from Refs. 121, 122, 123. These calculated fluxes are in the same order of magnitude that the Hg accumulated annually in shelf sediments (see Section 2.3.). This observation suggests that most of the Hg associated with riverine particles settles into shelf sediments.

For submarine groundwater discharges (SGD) the available data are even more limited. The Hg load of SGD has been studied in the Marseille region (NWMED)[124]:

THg concentrations were in the picomolar range and often < 3 pmol L^{-1}. (For a 20 km long coastline an annual mean of THg discharge of 0.14 ± 0.12 kg was calculated. Extrapolating this figure to the total MED shoreline and assuming constant submarine discharge point and flux density gives a total Hg flux from SGD of ~0.32 Mg y^{-1}. However, this figure could be largely underestimated. Trace element SGDs in the WMED have been estimated to be roughly in the same range as riverine discharges[125]. Assuming a similar behavior for Hg would give a total Hg discharge from submarine groundwaters an order of magnitude higher, namely ~6 Mg y^{-1}. In summary, Hg inputs from continental exoreic water sources to the MED can be estimated at ca. 12 Mg y^{-1}. Here again, this flux is not well constrained, and more studies are needed on rivers and especially SGD.

2.7. Mercury budget in the Mediterranean Sea

The diagram in Figure 6 sums up the Hg exchanges at the boundaries of the system and the Hg species inventory of the two MED basins. Precision concerning the Hg measurements, their natural variability, as well as that of the hydrodynamic and particulate fluxes, make this an exercise with major uncertainties. However, information that can be gained by such a mass balance calculation is to reveal the relative magnitudes of various sources and sinks and to test the hypothesis of a steady-state of Hg in the MED waters. In terms of balance, Hg output exceeds input by ~15 Mg y^{-1}, which is ~17% of the total export flux. Considering the uncertainties, the present Hg budget is close to balance. However, if we consider the excess of Hg export as real, this means that the Hg quantity in the MED is decreasing at the time scale of the residence time of Hg (2% y^{-1}). This is consistent with the observations of a ~30% decreasing Hg concentrations in the MED over the last 20 years[46].

In summary, the achievements of the updated budget are:

- It is confirmed that the exchanges between surface water and the atmosphere dominate the Mediterranean Sea Hg transport; however, the excess of evasion compared to the deposition, currently given by the models, is still insufficiently supported by the observations to be fully reliable;
- In absence of a robust quantification of diffusive Hg flux from sediment, the Hg buried in deep sediment is estimated around 5.8 Mg y^{-1};

- The Hg accumulation rate in shelf sediments is ~6.8 Mg y^{-1}, which is similar to the Hg flux from rivers; part of it is probably temporarily trapped in coastal sediments before a possible transfer to the deep sea *via* submarine canyons;
- The finding that Hg efflux to the Atlantic Ocean, with intermediate and deep waters at Gibraltar, dominates the Atlantic input in surface water (by a factor ~2), with Hg entering the MED as inorganic species and escaping substantially as MeHg; MED is a site of MeHg production and a point source of MeHg for the adjacent Northeastern Atlantic Ocean (~1.4 Mg y^{-1});
- The estimation of a Hg (MeHg) content of the MED ~680 Mg (~150 Mg), with 0.7% being associated with biota (6% of which is annually removed by fisheries) (see section 4 below);
- The estimation of a residence time of Hg in MED waters < 10 years, which is roughly 5 to 10-times less than the residence time of waters; thus, decreasing the atmospheric Hg deposition (i.e., a decrease of anthropogenic emissions) over the MED region would more rapidly decrease the Hg concentration in MED waters than in other parts of the World Ocean.

The present budget remains poorly constrained about several Hg inputs especially those from geotectonic origins, coastal erosion, SGD, sedimentary mobilization, and point sources. These uncertainties are added to that of the imbalance in the Hg air-sea exchanges between evasion and deposition. Seasonal variation of numerous inputs needs to be assessed. In addition, the transport of particulate Hg inputs from terrigenous origin to the deep open sea through canyons is not quantified. For example, which part of riverine Hg inputs (associated with particulate material) remains in the margin sediments, which part reaches the abyssal sediments *via* canyons or is released in the water column, and may become available to benthic food webs? Such questions need answers for refining the Hg budget in order to use it to manage the near-shore areas where fishing and aquaculture activities are located.

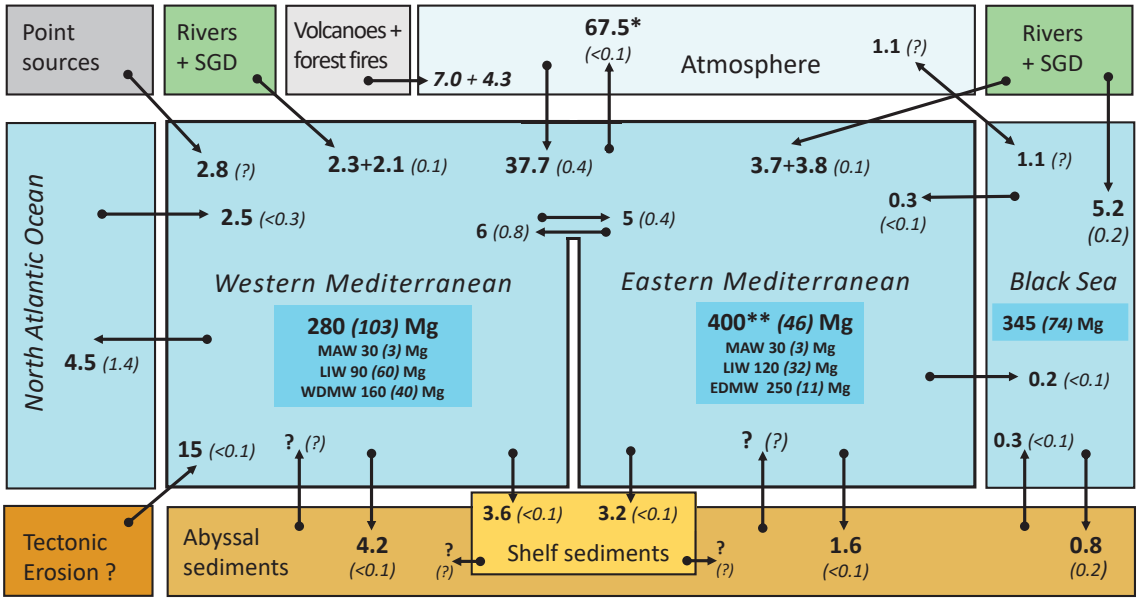

Figure 6. *Total Hg (THg in bold) and methylated Hg (MeHg in brackets) annual mass fluxes in the Mediterranean Sea (Mg y^{-1}). In the dark blue rectangle are the Hg inventories (Mg) in sub-basins and water masses. Fluxes from modeled air-sea exchanges are discussed in Section 2.1, Gibraltar exchanges are from Section 2.4, volcanic inputs from Section 2.5, and sediment deposition from Section 2.3; point sources are taken from Refs. 32, 33, 40, and 126; tectonic fluxes from Ref. 40 (probably an underestimation), are not differentiated according to basins; erosion fluxes are not quantified; fluxes from/to the Black Sea are from Ref. 45. The seawater fluxes at the Sicily Strait are from Ref. 123. Mediterranean areas and volumes are from Ref. 127. *Range: 50-100 Mg y^{-1}; **THg concentrations in the EMED used for calculation are limited to 24 measurements on only one profile in the Ionian Sea acquired in 2004 during MEDOCEANOR-3 cruise.*

3. Biological mercury transformations: state of the art for MED

The net amount of MeHg formed in the ocean is controlled by three processes: (i) the methylation of Hg_i^{II} to MMHg, (ii) MMHg demethylation to Hg_i^{II}, and (iii) interconversion between DMHg and MMHg. Abiotic methylation of Hg_i^{II} is possible if suitable methyl donors are present, but research efforts have mostly been concerned with biologically mediated Hg methylation. The biological methylation of Hg_i^{II} to MeHg can be performed by microorganisms carrying the *hgcA* and *hgcB* gene clusters[128, 129, 130, 131]. A detailed description of the gene clusters is given in Supporting Information (SI.5). Some *Nitrospina hgcA*-like genes in one of three MED water samples were also detected[132]. In particular, those gene copies were detected in surface waters and were not detected at the deep chlorophyll maximum of the MED. Three samples are not representative of the vertical and horizontal variability of the MED but, based on previous knowledge, it can be speculated that *hgcA* might be more abundant in surface waters and

at the OMZ of the MED. Due to the lack of data, a more extensive evaluation of the presence and activity of *hgcA* in the MED is needed to determine the position in the water column where these microorganisms are active, and thus responsible for biological MMHg formation in the MED water column, and to unveil their different metabolic capacities.

Besides the occurrence of potential Hg_i^{II} methylators in the ocean, the amount of Hg_i^{II} available for methylation plays an important role in determining the rate of this process. In this context, Hg_i^{II} reduction, which might decrease Hg_i^{II} bioavailability for methylation, and MMHg demethylation, which might increase it, are both critical processes to consider. Both Hg_i^{II} reduction and MMHg demethylation can be biotically[133, 134] and photochemically mediated[135, 136, 137, 138]. As mentioned above, although rates of photochemical transformations have never been reported for the MED, it is logical that these processes are limited to the photic zone and thus to the AW. Similarly, there is no information concerning biological Hg_i^{II} reduction. Two pathways of MMHg demethylation have been identified: an oxidative pathway yielding Hg^{II} and CO_2, and a reductive pathway yielding Hg^0 and CH_4. Since the Hg^0 produced from reductive demethylation can diffuse out of the cell, it has been proposed that reductive demethylation is a cellular detoxification mechanism[134], which would dominate at high Hg concentrations, whereas the oxidative pathway, which is an unknown, would be more important at low Hg concentrations[139]. MMHg demethylation is biologically mediated by the *mer* operon[134, 140]. Lastly, the interconversion between DMHg and MMHg is still poorly understood but has been suggested to be potentially abiotic[141, 142]. In the MED the lack of knowledge regarding metabolic pathways and the organisms involved in these processes has limited the possibilities to further understanding of Hg biogeochemical cycling.

4. Biological transfers in food webs

In the MED, top-predator fish often exceed EU regulatory Hg thresholds[75, 143, 144, 145, 146, 147, 148] and contribute to the increase in MeHg exposure of seafood consumers[10, 149]. Also, for over 50 years, Hg-enrichment in Mediterranean fish compared to other oceanic regions at the same latitudes has been observed[17, 18, 147], with the result that Aston and Fowler[20] describe these findings as a real “mercury enigma” in MED biota. After debates about the possible importance of biological factors[20, 75], a comparison of Hg content in

564 hake and its food web elements from the MED and the adjacent North Atlantic Ocean
565 suggests a multi-causal explanation for this issue[21], namely (i) the location of the MeHg
566 maximal concentration in the water column, (ii) the growth rates of the fish, and (iii) the
567 structure of the food webs.

568 Most available information on Hg concentrations in Mediterranean organisms, from
569 primary producers to marine mammals and birds, recorded between 1969 and 2015 was
570 compiled into a large database[148]. Among Animalia about 80% of samples concern
571 Actinopterygii (mainly teleost fish) and Bivalvia (mainly mussels), while among Plantae
572 87% of the data concern the seagrass *Posidonia oceanica*, highlighting the lack of
573 knowledge on Hg content in important small organisms, such as phytoplankton
574 producers, zooplankton consumers, and benthic invertebrates. More information is
575 available from the northern than the southern part of the MED and the western rather than
576 the eastern basin[148]. Hg transfer in biota involves three complex multifactorial processes
577 (bioconcentration, bioaccumulation, and biomagnification) interacting at different levels
578 of the food webs, which need to be taken into account for a true understanding of
579 Mediterranean specificities and to facilitate geographical comparisons.

580 ***4.1. Bioconcentration***

581 Bioconcentration is the absorption of contaminants in organisms directly from water
582 through cell membranes. This is the first and most important step in Hg transfer, which
583 occurs mainly at microorganisms levels. Bioconcentration depends not only on the
584 bioavailable Hg concentration in seawater, but also on the specific composition of
585 phytoplankton communities, their abundance, and size, which govern Hg sorption and
586 uptake in the first trophic level of food webs[150]. It has been demonstrated that MMHg is
587 preferentially integrated into the cell cytoplasm whereas Hg_i^{II} is adsorbed on
588 phytoplankton membranes[151]. As a consequence, MeHg is assimilated by zooplankton
589 four times more efficiently[150] than Hg_i^{II}. For a given Hg concentration in seawater,
590 absorption is negatively related to phytoplankton abundance (dilution by biomass), and
591 uptake is negatively related to cell size (higher surface/volume ratio in smaller cells) and
592 their rates vary among species[152, 153]. As the base of the food web is mainly made up of
593 pico- or nano-bacteria and phytoplankton in oligotrophic Mediterranean seawaters[154], the
594 combination of low phytoplankton abundance and small-sized cells increase both sorption
595 processes resulting in higher Hg concentrations of the first trophic level in the MED than
596 in the northeastern Atlantic[21]. At a smaller spatial scale in the MED, higher Hg

bioconcentration in phytoplankton is also found in oligotrophic offshore waters than in mesotrophic coastal waters due to similar processes[21]. In the MED, the higher proximity at mid-depth of both chlorophyll (~40 m)[155] and MeHg maxima (~250-400 m)[21] increases Hg bioavailability for phytoplankton incorporation. In contrast, these two zones are more separated in the Northeastern Atlantic, where the MeHg maximum is located in deep waters (800 m)[21] and the chlorophyll one in shallow waters (5-40 m), contributing to reduce bioconcentration at the base of the food webs in this region. In the Black Sea, MeHg maximum occurs in permanently anoxic waters[45]. The strong stratification of the water column between the oxic and anoxic layers precludes the exposure of higher living organisms to elevated MeHg concentrations. In addition, the high primary production of the Black Sea adds a bio-dilution effect and may contribute to explaining the lower Hg bioconcentration observed[156].

Studies in the Gulf of Lion provide evidence of higher Hg concentrations in the smaller (6-60 µm), rather than the larger (60-200 µm), phytoplankton fractions analyzed[157], consistently with the results obtained experimentally and by modeling[150, 158]. However, in these small-size fractions, detrital organic particles and numerous associated bacteria are mixed with autotrophic and heterotrophic plankton. That raises the question of the relative role of living and non-living particles, and of the different types of plankton in Hg transfer in food webs. Which species or size fractions are the most significant for Hg transfer in food webs? It seems that Hg could be more readily assimilated by copepods when they are feeding on ciliates (protozoa) than on phytoplankton or heterotrophic dinoflagellates[159].

4.2. Bioaccumulation

Bioaccumulation refers to a contaminant increase in an organism during its lifetime from both the environment and food consumption. Hg bioaccumulation in consumer organisms during their lifetime is mainly due to prey consumption[160, 161], and differs widely according to species, and the organs or body parts considered[148, 157, 162]. Thus, the Hg content of prey is one of the major parameters for explaining bioaccumulation in organisms, and a positive correlation between Hg content in food and consumer is generally observed[163]. In the MED as elsewhere, whole organisms are analyzed for plankton, benthic invertebrates, and fish larvae due to their small size, whereas muscle tissues are generally analyzed in larger marine consumers (crustaceans, cephalopods, and fish) due to their consumption by human populations[10, 146]. Other tissues are analyzed for

larger Mediterranean predators, such as skin biopsies for mammals[164] or blood for seabirds[165]. Higher Hg concentrations are generally found in the liver, compared to muscle and the gonads in MED fish[157, 166, 167], while this pattern may differ according to species, higher Hg content is found in muscle than liver of hake[168] and shark[169]. Conversely, a higher MeHg percentage (85-97%) is recorded in muscle than in the liver (30%)[162] due to the slower elimination rate from muscle than liver (2% and 60% respectively)[167]. In addition to organ differences, bioaccumulation is modulated at the individual level by a series of interacting biological (species, size, weight, sex, age, life duration, growth rate, reproduction, metabolism, proximal composition, detoxification mechanisms, diet, etc.) and environmental (depth, habitat, temperature, primary production, etc.) factors, as described in studies of the European hake *Merluccius merluccius*[21, 170, 171] and small pelagic fishes in the Gulf of Lion[157]. The synergistic and antagonistic effects of all these factors, which vary in space and time for a given species, explain the high variability of the vast amount of data published on Hg concentrations in MED organisms and the complexity of fully understanding and explaining local and regional differences (e.g., Ref. 148 and references therein). Generally speaking, a positive correlation is observed between Hg concentration and individual size, weight, age, trophic level and depth, and a negative correlation with growth rate (Hg dilution by an increase in organism biomass) in MED fishes and mammals, with numerous exceptions according to species or populations. For example, a higher Hg content was found in male than female hakes of similar size in the Gulf of Lion but not in the Bay of Biscay, as males grow more slowly than females in the MED, but not in the Atlantic[21]. Hg content was correlated with size in *Mullus surmuletus* in the Ligurian Sea[172] and south of Spain[168] but not in the Gulf of Lion[156]. A recent study also demonstrates the importance of the proximal composition (mainly protein and lipid contents) of organisms on Hg concentration in MED fish[168]. Besides, as the whole life history determines Hg accumulation in organisms, the inter-individual variability would be higher in the older, often also the larger, individuals in a population, a pattern observed in MED fishes[170, 173] and marine mammals[164]. Most authors agree however on the higher Hg bioaccumulation in MED benthic fish species compared to pelagic fish, and in individuals within species occurring at deeper than in shallower waters[, 166, 173, 174, 175, 176], while exceptions are also observed[177].

662 Regional comparisons of Hg concentrations in marine organisms are thus
663 complicated by the combination of the high number of factors involved in contaminant
664 bioaccumulation and may differ according to the organisms studied[178]. Mediterranean
665 organisms, from sponges to fish, marine mammals, and seabirds, are known for their
666 higher Hg concentrations than their Atlantic counterparts[21, 48, 164, 165, 179, 180, 181, 182] . Within
667 the MED, some geographic regions such as the North Adriatic Sea, the Tyrrhenian Sea,
668 and the Sea of Marmara[174, 180, 181] are known hotspots for Hg bioaccumulation, while the
669 Aegean Sea[183], Ionian Sea[174], the Black Sea[156], and the Tunisian coast[162] appear to be less
670 contaminated. Locally, Hg concentration in one species may vary by an order of
671 magnitude, as observed for mussels on French MED coasts[184]. The exceptionally high
672 spatial variability in MED organisms is highlighted by all studies, both between western
673 and eastern basins, northern and southern coasts, and among habitats and depths. An
674 example of the WMED-EMED difference of Hg content in fish is provided by the red
675 mullet *Mullus barbatus*, a much-used species in monitoring surveys, from the Gulf of
676 Lion[170] and the coast of Turkey[183]. *M. barbatus* of the same size range (11-19 cm TL)
677 exhibit a ~2 times higher mean Hg content in the WMED (0.190 ± 0.013 μg g^{-1} wet
678 weight in muscle, n = 94) than the EMED (0.090 ± 0.017 μg g^{-1} ww, n = 52) (Fig. 7). The
679 regression logHg *vs* size presents a significantly higher intercept in the WMED than in
680 the EMED, suggesting a higher Hg concentration at the base of the food web in WMED,
681 while slopes do not differ due to the high variance of data indicating similar Hg
682 bioaccumulation rates in the two fish populations. Such regional differences in fish Hg
683 content could be related to the higher MeHg concentration in WMED than EMED waters
684 (Fig. 3), which could induce more pronounced bioconcentration processes and thus
685 higher Hg content in all trophic levels in WMED food webs. Consistently, the relatively
686 high Hg bioaccumulation observed in Mediterranean hakes[21] could be essentially related
687 to the environmental specificities of the MED compared to the adjacent NE Atlantic,
688 including slightly higher MeHg concentrations in waters where predators are foraging.
689 This latter hypothesis is supported by recent results on bluefin tuna, for which very high
690 Hg levels have been observed[22]. Indeed, Tseng et al. (2021)[22] showed that this long-lived
691 apex predator has Hg accumulation rates (defined as a change in muscle Hg concentration
692 per unit change in either size/weight or age) which reach the highest level in the MED
693 and decrease as North Pacific > Indian Ocean > North Atlantic. The authors argue that the
694 Hg accumulation rate in tuna can be used as a Hg contamination index in the oceans. This

interesting hypothesis deserves further testing and it is probably related to the high methylation capacity of MED waters (see section 2.2.2).

In addition, the higher temperature of the MED and its oligotrophic waters would induce an increase in metabolic activity[185, 186] and a decrease in the growth of the organisms[187, 188], leading to a smaller size at a given age, which, along with a lower Hg elimination rate[167], would induce higher bioaccumulation of Hg in Mediterranean organisms[21, 48].

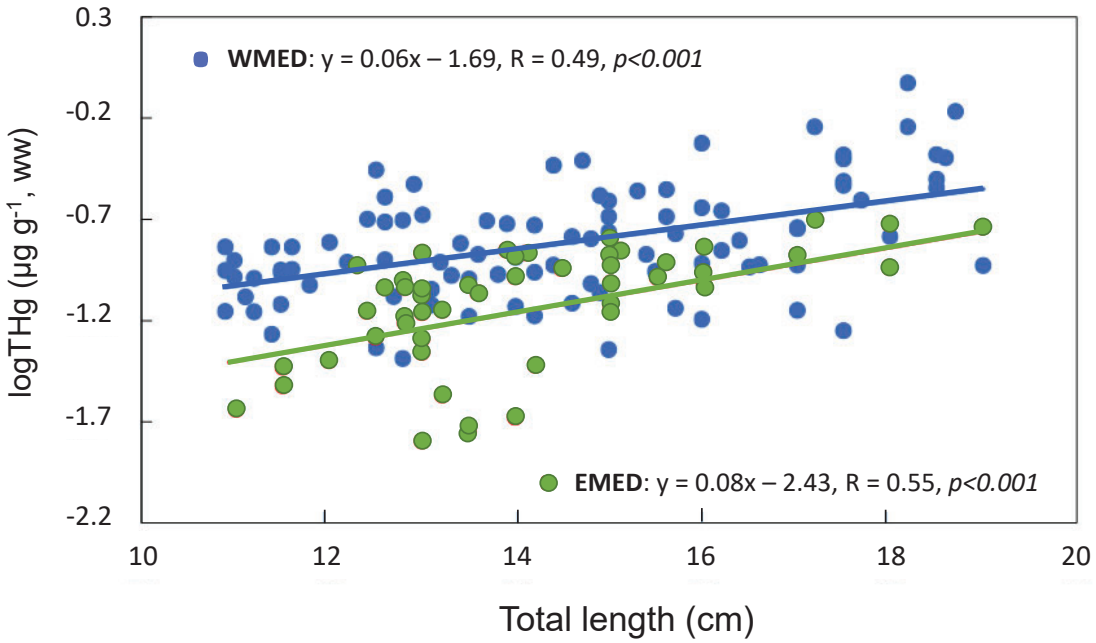

Figure 7. *Log-log relationships between THg and total length in the red mullet* (Mullus barbatus) *from the Gulf of Lion, France (WMED) and the Gulf of Izmir, Turkey (EMED).*

4.3. Biomagnification

Biomagnification is defined as the increase in Hg concentration in organisms from prey to predator throughout food webs from primary producers to high trophic level predators. Some studies provide data on Hg biomagnification along Mediterranean food webs from primary producers to various consumers at different trophic levels[21, 157, 176, 178]. Most often the food webs analyzed were comprised of only a few trophic levels as highlighted in the worldwide meta-analysis[189] in which the food webs analyzed ranged across a mean of only 1.7 trophic levels, but a few studies recently analyzed entire food webs from phytoplankton to marine mammals[153]. All studies provide evidence of an exponential

714 increase of total Hg concentration with the trophic level increase, and a steeper slope for
715 MeHg which presents a higher retention efficiency due to its lower elimination rate.

716 Mercury biomagnification in food webs is generally quantified either by the trophic
717 magnification slope (TMS) (also called biomagnification power), corresponding to the
718 slope (b) of the regression between logHg or logMeHg *vs* trophic level or $\delta^{15}N$ of the
719 organisms, or by the trophic magnification factor (TMF) calculated as $TMF = 10^b$ (see
720 Ref. 190 for a critical discussion). Trophic magnification slope generally ranges from
721 0.11 to 0.22 for total Hg, and from 0.14 to 0.36 for MeHg in the food webs studied from
722 polar to tropical ecosystems, which corresponded to TMFs ranging from 1.29 to 1.66 for
723 Hg and from 1.38 to 2.29 for MeHg[153, 184, 189]. The TMFs calculated for Hg in
724 Mediterranean food webs are within this range with a lower value in Sicily (1.22)[175] than
725 in the Gulf of Lion (1.68)[171] or the Bay of Marseille (1.25 - 1.58)[177], but reaches 2.40
726 (TMS = 0.38) for MeHg in the Gulf of Lion[21]. A higher biomagnification power for
727 MeHg was calculated in the hake food web in the MED than in the NE Atlantic (2.40
728 and 1.95 respectively)[21], while no difference in MeHg biomagnification power between
729 the MED and the Atlantic was found for deeper fish species occurring in deeper
730 waters[48], such as the sharks *Scyliorhinus canicula* and *Galeus melastomus.* Currently,
731 due to the scarcity of relevant data, it is not possible to account for a particular Hg
732 biomagnification in MED food webs. However, a possible hypothesis is that the smaller
733 size of individuals in the MED induces longer or more complex food webs, which may
734 result in a higher Hg biomagnification factor. It is proposed that longer food chains
735 induce a decrease in energy transfer and an increase in contaminant retention[191, 192].
736 During summer, when nutrients become limiting, changes in trophic conditions could
737 modify the importance of the microbial loop as well as the role played by mixotrophic
738 organisms in the trophic transfer of Hg. It is not known if there are differences in the
739 processes involved in Hg transfer and biomagnification in pelagic and benthic-
740 dominated food webs or a difference in the magnitude of similar processes. Few data are
741 available on Hg and MeHg concentrations in the benthic invertebrates which constitute
742 important prey sources for higher trophic level consumers. The specificity of the MED
743 food web functioning itself may well influence Hg transfer[193].

744 The use of different trophic markers (carbon and nitrogen stable isotopes, fatty acids,
745 amino-acids, compound-specific stable isotope analyses) and stable Hg isotopes may
746 improve the comprehension of trophic transfer in the first levels of the food web and

thus refine the estimation of Hg and MeHg transfers under varying environmental conditions. Ecosystem models such as ECOPATH with ECOSIM, ECOSPACE, and ECOTRACER[194, 195] take into account all food web interactions. Applying such models here should allow better quantification of the trophic transfers of Hg and MeHg in MED ecosystems and their temporal and spatial variability. Regional food web models accounting for bioaccumulation need to be implemented to simulate the spatial variability, as well as the population-variability, of Hg concentration in organisms, and refine the estimation of total Hg and MeHg content in MED biota. All these questions require accurate knowledge of organism biology, physiology, and ecology, to determine how they differ in the MED from adjacent areas.

4.4. Quantification of Hg content in Mediterranean biota and fisheries harvest

From the data compiled in the Supporting Information (SI.6), we estimated the THg and MeHg content in MED biota. Detailed methodological and calculation details are also given in the Supporting Information (SI.7). The estimate indicated that MED marine biota contains ~ 4.7 Mg of THg and ~2.2 Mg as MeHg. Due to the uncertainty associated with the initial biomass estimation, a range between 3.0 and 6.4 Mg of THg in MED biota can be approximated using the standard deviation of the biomass compartments[196]. These results illustrate not only the importance of primary producers, which represent 13% of THg in MED biota, as already observed in other mass balance inventories[197] but also the chief importance of the benthos, a too often neglected compartment, which accounts for ~50% of THg (32% of the MeHg) in MED biota. Cetaceans also constitute an important Hg reservoir (10% of THg and 18% of the MeHg present in MED biota). However, THg in biota represents only a small part (0.7%) of the general Hg budget in the MED. An estimation of Hg removed from the MED by fishery catches was performed using the observed data of catches for the year 2011[196]. A total of 0.30 Mg THg y^{-1} and 0.26 Mg MeHg y^{-1} is extracted from the MED by fisheries, which is similar to the value of 0.29 Mg MeHg y^{-1} calculated by Žagar et al.[41] using a different method. However, in contrast to these authors, total aquaculture products were not included in our estimation, which could therefore be considered as a minimum value. Catches therefore annually remove ~6% of the THg and ~12% of MeHg held in living biomass in the MED. Sharks and small pelagic fishes (including sardine and anchovy) constitute the main quantities of MeHg (20% each) removed by MED fisheries, followed by large pelagic (13%) and large

779 demersal (11%) fishes. These estimations should be treated with caution as a large degree
780 of uncertainty is associated with all steps of the calculations.
781
782 **5. Human exposure**

783 Mercury is one of the ten most important pollutants of global concern for human
784 health[198]. The major toxic effects of MeHg, a naturally occurring organic form of Hg
785 prevalent in fish, are on the central nervous system, with the developing fetus being
786 most vulnerable[1, 3]. The consumption of fish is considered a major source of Hg
787 exposure to humans. Other sources are well described, but their contributions are minor
788 in comparison with fish consumption[199].

789 Human exposure to Hg and its compounds can be assessed through the
790 measurement of Hg concentrations in many different biological sample types. The most
791 commonly used biomarkers are the concentrations of mercury in hair, urine, blood, and
792 cord blood, and their selection can depend on factors such as the potential source of
793 exposure, chemical form, and exposure life stage. An extensive recent review indicated
794 that the individuals with the highest reported Hg levels were those living in the Arctic,
795 Pacific, MED, and Atlantic coast regions who consume the highest amounts of fish,
796 seafood, and marine mammals[200]. It has been shown that several species of fish from the
797 MED have higher levels of Hg in their tissues compared with the same species from the
798 Atlantic Ocean[201, 202,] and references cited in section 4.3. An extensive review of
799 mercury levels in biota is presented by Cinnirella et al.[148] and indicates that among all
800 the species considered, *Diplodus sargus*, *Sardina pilchardus*, *Thunnus thynnus,* and
801 *Xiphias gladius* show trends of mercury concentration higher than safe limits defined by
802 WHO and EU.

803 Human exposure to Hg in Europe, and in particular, the question of whether MED
804 populations are more exposed to this contaminant than other European populations has
805 been addressed in the literature. Two studies have evaluated Hg concentrations in blood,
806 urine, and hair, widely used biomarkers to evaluate Hg human exposure, of populations
807 from European Countries[199, 203]. Both studies agreed on the fact that there are significant
808 differences in MeHg exposure across the EU and that exposure is highly correlated with
809 the consumption of fish and marine products, as well as the availability of large fish
810 species from the MED. Whether human exposure to Hg is higher in the MED than in

North European countries still needs to be elucidated through a well-designed comparative study.

The results of studies in the MED countries are provided in the Supporting Information (SI.8)[199, 203]. The highest levels are found in coastal regions with local seafood consumption (Spain, Morocco, Tunisia, and Greece) which is consistent with other studies around the world. In the framework of the EU-funded DEMOCOPHES project[204], the dietary habits and consumption frequency of fish and other marine products showed great variations among the 17 EU countries, which was also reflected in the high variability of Hg levels in the hair of mothers and children. Among the MED countries participating in DEMOCOPHES the highest values (geometric means) were found in Spain (1.59 μg g^{-1}), whereas Cyprus and Slovenia showed much lower values (0.43 μg $g^{-1}$and 0.26 μg g^{-1}, respectively).

In the MED region, two cohort studies aimed to link prenatal Hg exposure and health outcomes in newborns. The prenatal exposure in both studies was based on cord blood mercury measurements. In Spain, the "Environment and Childhood" (INMA) study implemented in the period 2004 to 2008 included several regions, and 1883 cord blood samples were analyzed for THg[205]. The highest concentrations expressed as geometric means were found in samples collected in Valencia (9.5 μg L^{-1}) and Asturias (10.8 ng mL^{-1}) and were strongly related to fish consumption, especially large oily fish and tuna. The second MED cohort study included coastal regions in Italy, Slovenia, Croatia, and Greece[206, 207] in the period between 2007 and 2011. This cohort study included 1308 mother-child pairs enrolled in the Public Health Impact of long-term, low-level, Mixed Element exposure in a susceptible population (PHIME). The highest levels of cord blood samples were found in the Greek population with geometric means of 7.7 ng mL^{-1}, followed by Italy with 5.6 ng mL^{-1}, Croatia with 5.1 ng mL^{-1}, and the lowest in Slovenia with 2.1 ng mL^{-1}. These levels were strongly correlated with fish consumption, and in Greece primarily due to locally caught fish. The Valencia and Asturias region in the INMA and Greek PHIME prenatal exposure values are comparable to regions with high fish intake in Japan, Honk Kong, Korea, and Polynesia[205]. These two studies confirm the data presented in Supporting Information (SI.8) that indicate high variability of Hg exposure in the MED region reflecting variation in the frequency of fish consumption, their sources, and type. Similar findings were reported in a recent publication[10], where mean Hg levels in hair for women of childbearing age on the French Mediterranean

844 coast were higher than for women of childbearing age from other European countries.
845 This trend is in accordance with the higher annual fish consumption *per capita* in
846 various European countries. Besides, it has to be noted that fish from aquaculture often
847 have lower Hg levels compared with wild fisheries. For example, levels of Hg in seabass
848 (*Dicentrarchus labrax*) from wild fisheries in the MED were, on average, approximately
849 10 times higher than in aquaculture seabass[207].

850 While fish consumption is an important element of human health, especially in the
851 early stages of life[208, 209], higher MeHg exposure during pregnancy is associated with a
852 poorer metabolic profile. Both MED epidemiological studies, INMA and PHIME, also
853 indicated that there is a growing awareness of inter-individual differences in the
854 toxicokinetics of Hg and the resulting biomarker measurements may be influenced by
855 genetic polymorphisms[210, 211]. Since the symptoms of MeHg exposure are subtle and
856 multi-causal, there is still no consensus on a health-based guidance value for MeHg
857 exposure despite the large number of studies trying to connect low exposure levels to
858 actual risk[209, 212]. However, there is a general recommendation that pregnant women,
859 children, and women of childbearing age should be protected as much as possible from
860 Hg exposure. Therefore, it is important to know what the actual exposure to MeHg is in
861 the general population and what the sources of exposure are to formulate adequate
862 mitigation strategies and recommendations. For example, an attempt was made for the
863 Italian population[213] with the formulation of advice regarding food habits that could
864 maximize the benefits, whilst reducing the risks of MeHg intake in sensitive groups
865 without compromising seafood consumption. This should allow a better understanding
866 of the food risk associated with mercury, particularly in highly polluted sites. Overall,
867 the Minamata Convention on Mercury sets guidelines for limiting human exposure to
868 Hg. Article 22 of the Minamata Convention calls for parties to monitor mercury in the
869 environment as well as in people (biomonitoring) as a way of assessing the effectiveness
870 of the convention.

871

872 **6. Modeling the Hg cycle in the Mediterranean**

873 Numerical biogeochemical models are effective tools to investigate the fate and
874 transport of Hg in the environment. Synthesizing available knowledge into a rigorous
875 framework, they help to highlight gaps in process understanding and data availability[32,
876 33, 45, 214, 215, 216, 217, 218, 219, 220, 221, 222, 223]. Moreover, models can be used to predict the

877 evolution of a system under different Hg emission scenarios, trophic conditions, and
878 climate change, supporting the evaluation of alternative management strategies[218, 219, 224,
879 225, 226, 227]. Reviewing modeling studies for the marine Hg cycle in the Mediterranean
880 area, we found that only one paper has sought to model the Hg cycle in the MED at the
881 basin scale[41], pointing out uncertainties in Hg input to the basin and a poor
882 understanding of Hg methylation and demethylation processes at that time. Other
883 modeling efforts in the MED are local scale studies focusing either on transport and
884 transformation processes of Hg species in regional seas[69] and coastal sites[32, 224, 228, 229,
885 230, 231], as well as on the bioaccumulation and biomagnification processes[21, 232]. Most of
886 these models still presented several limitations, namely, the use of the quasi-steady state
887 approach, coarse spatial resolutions, and the lack of full coupling between physical and
888 biogeochemical processes.

889 Small-scale assessments are relevant to provide estimates of Hg fluxes from coastal
890 and former industrial areas[233] since a comprehensive assessment of Hg point sources and
891 legacy Hg for the MED is lacking. However, existing modeling studies for Hg in the
892 MED are also geographically biased as they have been carried out in the areas where
893 more data have been collected over the years: either the Northern Adriatic Sea, or the
894 NWMED. Significant differences in the distribution and fluxes of Hg species are
895 observed[46, 88] in these two sub-basins, driven by contrasting oceanographic and
896 biogeochemical features, (i.e. the Northern Adriatic Sea is a shallow shelf with depth <
897 50 m and high river discharge, while the NWMED a deep system with seasonal
898 upwelling events), but a complete understanding of the MED system as a whole is
899 missing.

900 Remarkable research efforts in the last decades to unveil the mechanisms
901 underlying Hg methylation in the ocean pointed out organic matter remineralization as a
902 key process that triggers the release of dissolved Hg and fuels the activity of
903 heterotrophic bacterioplankton[96, 97, 234 , 235, 236]. Phytoplankton phenology patterns have a
904 large impact on MeHg production and bioaccumulation, as the cell size affects both the
905 ability to bioaccumulate Hg[152,158] and the sinking velocity after death, with small slow-
906 sinking plankton favoring water column Hg methylation in the water column[91, 237], and
907 large fast-sinking plankton acting as a fast vector for Hg sequestration through
908 scavenging and transport to the seafloor[238]. These pieces of evidence are fostering new
909 efforts aimed at developing integrated modeling tools that couple the biogeochemistry of

910 Hg species with that of organic matter and nutrients and with hydrodynamic transport[219, 223]. At the state of the art, coupled physical-biogeochemical models for the MED can simulate the key processes of nutrients (i.e., nitrogen, phosphorus, silica, iron) carbon, and oxygen in the water, sediments, and in the food web from heterotrophic bacteria to phytoplankton and zooplankton, reproducing the observed spatial gradient and seasonal variations of chlorophyll and primary production at a spatial resolution up to 1/64 degree[239]. Validated model outputs for the OGSTM-BFM model, a biogeochemical model coupled to the physical model NEMO-OceanVar, are freely available at the Copernicus Marine Service site (https://resources.marine.copernicus.eu), with a spatial resolution of 1/24 degree, for 125 depth levels, for forecast simulations and 20-year reanalysis. Given the high standard attained in physical-biogeochemical models, a full physical-biogeochemical-Hg coupling will likely add insights into the cycling of Hg in the MED and its possible future evolution.

923 To improve our ability to model the Hg cycle, a better mechanistic understanding is also needed. A few measurements are available for Hg methylation and demethylation rates in the MED waters, as well as for the formation of Hg^0 and DMHg[43, 44, 240]; but rates of photochemical transformations have never been assessed in the MED[137, 138], nor has a full mechanistic understanding been achieved for any of these processes. Moreover, a recent review highlighted significant uncertainties in assessing potential seawater Hg methylation and demethylation rates[241]. Given the relevance of DMHg in the open ocean[39, 43], more observations and modeling experiments are needed to constrain transformation kinetics between DMHg, MeHg, and divalent Hg_i[237]. Further investigation of Hg species transformations in sub-basins of the MED with different trophic status could provide more reliable site-specific rates to be used in the models and could help to elucidate how different controlling factors, such as primary production, dissolved organic matter, oxygen, temperature, and chlorides affect transformations kinetics. The continuous availability of data of Hg species in water and plankton, the latter being particularly scarce in MED[148], is also crucial for model validation and to improve our ability to deal with the challenges posed by climate change.

939

940 **7. Overview of recent advances**

Compiling the oceanographically consistent THg data obtained in the open WMED waters between 2000 and 2017 allowed us to draw a consistent pattern of Hg distributions (Fig. 2). The THg concentrations of the upper layer (AW) are rather variable (as a result of Hg evasion and biological pumping) averaging 0.86 ± 0.27 pmol L^{-1}, whereas, in the intermediate and deep waters (EIW+WMDW), they are more homogenous with a mean of 1.02 ± 0.12 pmol L^{-1}. In the EMED, the available THg measurements are in the same range as those of the WMED but are far too few to determine any consistent oceanographical pattern. MeHg represents around 10, 40, and 13% of THg in AW, EIW, and DMW, respectively. The highest MeHg values are found in the OMZ with high AOU (Fig. 4). The methylating, *hgcA*-like genes from different microbial groups have even been identified in MED waters. The MeHg distribution seems likely to be ultimately governed by the intensity of primary production and the associated OM degradation. Consistently, MeHg concentrations in the mesotrophic WMED average twice those in the oligotrophic EMED. In addition, the methylation capacity of MED waters is high compared to other parts of the World Ocean. The THg (MeHg) inventories in waters are ~280 (100) Mg and ~400 (50) Mg for the WMED and EMED, respectively. Air-sea exchanges dominate the Hg fluxes, and Hg evasion largely exceeds atmospheric deposition (~30 Mg y^{-1} net). However, the excess of evasion, given by the models, is still insufficiently supported by the observations to be fully reliable. The MED is a net exporter of Hg to the adjacent Atlantic Ocean (~2 Mg y^{-1}, with ~1.4 Mg y^{-1} as MeHg), and MED abyssal sediments are a net sink for Hg (~6 Mg y^{-1}), whereas shelf sediments retain (at least temporarily) ~7 Mg y^{-1}. Most of this latter input originates from rivers (~6 Mg y^{-1}). This budget is, however, still far from being well constrained. For example, our estimations of submarine groundwater discharges, coastal erosion, submarine tectonic inputs, and point sources are rather coarse. High Hg concentrations were observed in Mediterranean predator organisms.

The MED is not only a bioreactor for MeHg production but also one of the places in the World Ocean where the methylation capacity of the Hg is highest. The difference in MeHg water concentrations between the MED basins (and other oceanic basins) appears to be transferred through the food webs and the Hg content in predators to be ultimately controlled by the MeHg concentrations of the waters of their foraging zones. Mediterranean top-predator fish still exceed European Union regulatory Hg thresholds. Since fish are the main vector of MeHg to humans, the current knowledge of the actual

974 exposure of MED populations to MeHg needs further consideration to formulate
975 adequate mitigation strategies and recommendations without compromising seafood
976 consumption. Mitigation of MED ecosystem exposure to Hg requires a full coupling of
977 physical-biogeochemical-Hg models based on a better assessment of anthropogenic Hg
978 sources; such coupling will likely add insights into the possible future evolution of the
979 Hg cycling in the MED, as a result of climate changes and variations in Hg atmospheric
980 deposition.

981

982 **8. Perspectives**

983 ***8.1. Hg cycle, climate change, and human coastal management in the MED***

984 MED shares most of the uncertainties with other parts of the global ocean concerning the
985 Hg cycle and its possible modification due to climate change. Non-Mediterranean-
986 specific changes in Hg cycling are expected from climate change, such as those listed for
987 a global perspective[242], including changes in atmospheric Hg oxidation and deposition
988 and wildfires. Also, climate change is expected to induce modifications in the
989 hydrological regime that would consequently affect the Hg atmospheric wet depositions,
990 input regime from rivers, and submarine groundwater discharges. More specifically, the
991 MED is very vulnerable to future climate change scenarios[28], which are expected to
992 induce an increase in vertical stratification, a depletion of oxygen in deep layers, and a
993 reduction of primary productivity. Shallow and deep-water mixing would affect the
994 efficiency of Hg transfer to the bottom sediments. A possible decrease in plankton
995 productivity may slow down the uptake and subsequent Hg scavenging. Depletion of
996 oxygen may favor the MeHg formation. However, the multi-causal drivers of Hg
997 methylation and demethylation rates add complexity to any attempts to predict future
998 effects. Besides, a reduction in European atmospheric emissions would lead to a decrease
999 in Hg deposition to the MED, and the short Hg residence time in waters should favor a
1000 rapid decline of Hg concentrations in waters. Climate change may induce in the MED not
1001 only a reduction of primary productivity but changes in phytoplankton community
1002 composition and likely a decrease in cell size, as already observed in different geographic
1003 zones[243, 244, 245]. Human coastal management may also impact terrestrial inputs, such as
1004 the decrease of phosphorus inputs to the Mediterranean rivers in recent decades inducing
1005 a decrease in plankton size[246]. An increase in oligotrophy and a decrease in cell size may
1006 thus increase Hg bioconcentration processes at the base of food webs. At higher trophic

levels, an increase in temperature would increase the metabolic demand of organisms[186] and affect their behavior[185], leading to a decrease in their growth rate and size that could cause an increase of MeHg bioaccumulation and a decrease in its elimination rate[167]. A decrease in organism size generally leads to longer and less efficient food webs, along which Hg biomagnification would be increased, while the effects of temperature on food web length are complex and may vary spatially[192, 247, 248]. Thus, the three Hg transfer processes in biota, bioconcentration, bioaccumulation, and biomagnification could be enhanced by different climate change scenarios in the MED[158], but its intensity would probably be highly spatially heterogeneous. An increase in Hg concentrations in marine organisms would be problematic for seafood consumers in the MED region.

8.2. The unknowns of the Mediterranean Hg cycle and research needs

Despite the numerous scientific advances described in this review paper, several uncertainties in the MED Hg distribution, cycling, and budget persist.

- Measurements of THg and MeHg in the Southern MED and the Levantine Basin waters are insufficient for mapping oceanographically consistent distributions of Hg species in the water column of the EMED.
- The revised Hg budget for the MED remains poorly constrained relatively to several Hg inputs especially because of the almost total absence of spatial and seasonal data series, including speciation, and fluxes at the air-sea interface, hydrothermal vents, cold seeps, SGD, and point sources. Monitoring systems for seasonally quantifying continental inputs have to be implemented.
- Notwithstanding a general agreement for a net Hg evasion flux (~30 Mg y^{-1}) to the atmosphere, taking into account the photolytic reduction of Hg^{II} compounds in the atmosphere could modify this figure. Gas-phase reduction of Hg^{II} would reduce dry and wet deposition to the MED, however by how much, requires further modeling studies to be performed. In addition, at-sea monitoring of seasonal and spatial variability (coastal upwelling) of Hg deposition and evasion is needed to explore to what extent atmospheric deposition is the primary factor controlling evasion of Hg^0 to the atmosphere. Such data will provide the basis for models and for validating them.
- The transport of particulate Hg inputs from terrigenous origin to the open sea through canyons is not adequately quantified. For example, which part of riverine Hg inputs (associated with particulate material) remains in the margin sediments,

which part reaches the abyssal sediments *via* canyons, which part is released in the water column, and which part may become available to benthic food webs?

- Some aspects of Hg speciation in waters are still questionable. For example, published observations on MMHg/DMHg ratios diverge widely in space and time and show little coherence or rationale. The ratio between the two methylated forms has consequences for MeHg fate and distribution between the atmosphere, water, and biota.
- Further work is also needed to elucidate Hg methylation mechanisms. The biogeochemical factors which promote net Hg methylation are still being identified. The importance of the nutrient status (and associated plankton communities) appears to be a determining criterion. Indeed, we know that the oligotrophic EMED waters are less loaded with MeHg than the WMED. To what extent is the heterotrophic activity responsible for Hg methylation, especially in phosphate-limited environments? Is there a place for abiotic methylation?
- The main challenge to advancing the understanding of Hg transfer in MED marine food webs resides in the clarification, and quantification, of bioconcentration processes at the base of the food chain, by far the largest "quantum" leap in Hg concentration in biota. This challenge comes with several questions:
    - What are the relative roles of food web length, plankton size and nature, and detritus in the transfer efficiency of MeHg?
    - How would differences in biomass of the various groups of viruses, bacteria, autotrophic and heterotrophic pico, and nanoplankton cells affect Hg bioaccumulation in zooplankton consumers?
    - Could the oligotrophic conditions modify the importance of the microbial loop as well as the role played by mixotrophic organisms in the trophic transfer of Hg?
    - Rather few data are available on Hg and MeHg concentrations in the benthic invertebrates which constitute important prey sources for higher trophic level consumers. Are there different processes involved in Hg transfer and biomagnification in pelagic and benthic-dominated food webs?

To sum up, a strategy for building a comprehensive understanding of the Hg cycle in the MED, allowing future assessment of global change impacts in conjunction with

the Minamata Convention Hg policy, should be based on long-term time-series observations, the use of new markers (e.g., Hg isotopes), and high-resolution Earth System Models dedicated to the MED area. Understanding, representing, and quantifying the interlinked processes involved in the Hg cycle, from earth system physics to microbial transformations, is far from trivial. Although the levels of uncertainty associated with individual processes are still high, models can be useful in dealing with such uncertainty through scenario analyses[45, 78, 224]. Coupled physical-biogeochemical numerical models can help in investigating the impacts of climate change on marine ecosystems focusing on Hg biogeochemistry and its interconnections with transport and transformation phenomen[33, 218, 219, 224] allowing different hypotheses and scenarios to be tested. Future efforts should be made in coupling Hg models into integrated regional and/or earth system models, able to describe Hg cycling through the ocean, atmosphere, and biosphere, and to properly consider contamination hot spots, and impacts on regions of particular interest, such as coastal areas[249, 250]. Such a challenge calls for a combination of modeling refinement, from the use of variable spatial mesh and/or downscaling, to a better parameterization of transport and transformation processes, aerosols, and Hg bioaccumulation and magnification in terrestrial and marine ecosystems. Such integrated modeling is the ultimate step in building realistic scenarios of Hg cycle evolution in the Mediterranean environment. New spatial and dynamic end-to-end ecosystem modeling which relates trophic transfer to Hg and MeHg transfer based on field data should be developed to relate observations of physical and biogeochemical processes to marine resource exploitation and consumption. Such integrated models are required to test scenarios and to be used as mitigation and management tools.

ACRONYMS

AOU: Apparent oxygen utilization
AW: Atlantic Water
DGM: Dissolved gaseous mercury
DMHg: Dimethyl mercury
DMW: Deep Mediterranean Water
EIW: Eastern Intermediate Water
EMED: Eastern Mediterranean
EU: European Union
GEM: Gaseous elemental mercury
GMA: Global mercury assessment

GMOS: Global mercury observation system
GOM: Gaseous oxidized mercury
Hg: Mercury
INMA: Environment and Childhood Project (ISGlobal, Spain)
MED: Mediterranean
MeHg: Methylated mercury (MMHg+DMHg)
MMHg: Monomethyl mercury
NWMED: Northwestern Mediterranean
OGSTM-BFM: OpenGeoSys Transport Model-Biogeochemical Flux Model
OM: Organic matter
OMZ: Oxygen minimum zone
PHIME: Public Health Impact of Long-Term, Low-level Mixed Element Exposure in Susceptible Population Strata (USA Department of Agriculture)
SGD: Submarine groundwater discharge
TDW: Tyrrhenian Deep Water
TMF: Trophic magnification factor
TMS: Trophic magnification slope
UNEP: United Nations Environment Programme
WHO: World Health Organization
WMDW: Western Mediterranean deep water
WMED: Western Mediterranean

Supporting Information

SI.1. Summary of the biogeochemical Hg cycle; SI.2. Calculation of the gas transfer velocities at the Mediterranean air-sea interface; SI.3. Summary statistics on total Hg concentrations in the western Mediterranean waters; SI.4. Methylated mercury in various oceanic basins; SI.5. Biological methylation and demethylation mechanisms; SI.6. Calculations of total and methylated Hg masses in Mediterranean marine biota; SI.7. Total and methylated Hg content in Mediterranean biota; SI.8. Mercury levels in exposure biomarkers in humans in the Mediterranean countries.

ACKNOWLEDGEMENTS

This research has been funded by the Global Mercury Observation System (GMOS, N-265113 European Commission project), and the European Research Council (ERC-2010-StG-20091028). The authors acknowledge the financial support from the project Integrated Global Observing Systems for Persistent Pollutants (IGOSP) funded by the European Commission in the framework "The European network for observing our changing planet (ERA-PLANET)" program, Grant Agreement: 689443. This work also received support from the MISTRALS transversal action on pollutants and contaminants

(INSU-CNRS). Thanks are due to M. Coquery for providing unpublished MeHg values from deep Mediterranean sediments, M. Petrova for THg concentrations in SGDs of Marseille region (France), and I. Taupier-Letage for her guidance in preparing figure 1.

References

[1] *UN-Environment. Global Mercury Assessment 2018*. United Nation Environmental Programme, Chemicals and Health Branch, Programme Chemicals and Health Branch Geneva Switzerland. 2019; www.unenvironment.org/resources/ publication/global-mercury-assessment-2018.

[2] Boening, D. W. Ecological effects, transport, and fate of mercury: a general review. *Chemosphere* **2010**, *40*, 1335-1351 ; DOI 10.1016/S0045-6535(99)00283-0.

[3] Chen, C. 2012. Methylmercury Effects and Exposures: Who Is a Risk? *Environ. Health Perspect.* **2012**, *120*, A224-225 ; DOI 10.1289/ehp.1205357.

[4] Eagles-Smith, C. A.; Silbergeld, E. K.; Basu, N.; Bustamante, P.; Diaz-Barriga, F.; Hopkins, W. A.; Kidd, K. A.; Nyland, J. F. Modulators of mercury risk to wildlife and humans in the context of rapid global change. *Ambio* **2018,** *47*, 170–197 ; DOI:10.1007/s13280-017-1011-x.

[5] Clarkson, T. W. The Three Modern Faces of Mercury. *Environ. Health Perspect.* **2002**, *110,* 11-23 ; DOI 10.1289/ehp.02110s111.

[6] *National Research Council, USA. Toxicological Effects of Methylmercury.* National Academy Press, Washington, DC 20055, USA**. 2000**. ISBN-10: 0-309-07140-2. https://www.nap.edu/read/9899.html.

[7] Roman, H. A.; Walsh, T. L.; Coull, B. A.; Dewailly, É.; Guallar, E.; Hattis, D.; Mariën, K.; Schwartz, J.; Stern, A. H.; Virtanen, J. K.; Rice, G. Evaluation of the Cardiovascular Effects of Methylmercury Exposures: Current Evidence Supports Development of a Dose–Response Function for Regulatory Benefits Analysis. *Environ. Health Persp*. **2011**, *19*, 5 ; DOI 10.1289/ehp.1003012.

[8] Bradley, M. A.; Barst, B. D.; Basu, N. A Review of Mercury Bioavailability in Humans and Fish. *Int. J. Environ. Res. Public Health* **2017**, *14*, 169-189 ; DOI 10.3390/ijerph14020169.

[9] Debes, F.; Budtz-Jorgensen, E.; Weihe, P.; White, R. F.; Grandjean, P. 2006. Impact of prenatal methylmercury exposure on neurobehavioral functions at age of 14 years. *Neurotoxicol. Teratol.* **2006***, 28*, 536-547 ; DOI 10.1016/j.ntt.2006.02.005.

[10] Petrova, M. V.; Ourgaud, M.; Boavida, J. R. H.; Dufour, A.; Tesán Onrubia, J. A.; Lozingot, A.; Heimbürger-Boavida, L.-E. 2020. Human mercury exposure levels and fish consumption at the French Riviera. *Chemosphere* **2020***, 258*, 127232 ; DOI 10.1016/j.chemosphere.2020.127232.

[11] Driscoll, C. T.; Mason, R. P.; Chang, H. M.; Jacobs, D. J.; Pirrone, N. Mercury as a Global Pollutant: Sources, Pathways an Effects. *Environ. Sci. Technol.* **2013***, 47*, 4967-4983 ; DOI 10.1021/es305071v.

[12] Lamborg, C.; Bowman, K.; Hammerschmidt, C.; Gilmour, C.; Munson, K.; Selin, N.; Tseng, C.-M. Mercury in the Anthropocene Ocean. *Oceanography* **2014**, *27*, 76–87 ; DOI 10.5670/oceanog.2014.11.

[13] Outridge, P. M.; Mason, R. P.; Wang, F.; Guerrero, S.; Heimbürger-Boavida, L.-E. Updated Global and Oceanic Mercury Budgets for the United Nations Global Mercury Assessment 2018. *Environ. Sci. Technol.* **2018**, *52*, 12968–12977 ; DOI 10.1021/acs.est.8b04542.

[14] Martinez-Cortizas, A.; Pontevedra-Pombal, X.; García-Rodeja, E.; Nóvoa-Muñoz, J. C.; Shotyk, W. Mercury in a Spanish Peat Bog: Archive of Climate Change and Atmospheric Metal Deposition. *Science* **1999**, *287*, 939-941 ; DOI 10.1126/science.284.5416.939.

[15] Streets, D. G., Horowitz, H. M.; Lu, Z.; Levin, L.; Thackray, C. P.; Sunderland, E. M. Global and regional trends in mercury emissions and concentrations, 2010–2015. *Atmos. Environ*. **2019**, *201,* 417-427 ; DOI 10.1016/j.atmosenv.2018.12.031.

[16] Streets, D. G., Horowitz, H. M.; Lu, Z.; Levin, L.; Thackray, C. P.; Sunderland, E. M. Five hundred years of anthropogenic mercury: spatial and temporal release profiles. *Environ. Res. Lett*. **2019,** *14*(8), 084004 ; DOI 10.1088/1748-9326/ab281f.

[17] Thibaud, Y. Teneur en mercure dans quelques poissons de consommation courante. *Sciences et Pêches, Bull. Inst. Pêches marit.* **1971**, XXII-XIII 79, pp. 10.

[18] Bernhard, M.; Renzoni, A. Mercury concentration in Mediterranean marine organisms and their environment: Natural or anthropogenic origin. *Thalassia Jugoslavica* **1977**, *3*, 265–300.

[19] Renzoni, A.; Bernard, M.; Sara, R.; Stoeppler, M. Comparison between the Hg body burden of *Thynnus thynnus* from the Mediterranean and the Atlantic. IVème Journées d'Etude de la Pollution, Antalya, CIESM, Monaco, 255, **1979**.

[20] Aston, S. R.; Fowler S. W. Mercury in the open Mediterranean: evidence of contamination. *Sci. Total Environ*. **1985**, *43*, 13-18 ; DOI 10.1016/0048-9697(85)90028-2.

[21] Cossa, D.; Harmelin-Vivien, M.; Mellon-Duval, C.; Loizeau, V.; Averty, B.; Crochet, S.; Chou, L.; Cadiou, J.-F. Influences of Bioavailability, Trophic Position, and Growth on Methylmercury in Hakes (*Merluccius merluccius*) from Northwestern Mediterranean and Northeastern Atlantic. *Environ. Sci. Technol.* **2012***, 46*, 4885-4893 ; DOI 10.1021/es204269w.

[22] Tseng, C. M.; Ang, S. J.; Chen,Y. S.; Shiao, J. C.; Lamborg, C. H.; He, X.; Reinfelder, J. R. Bluefin tuna reveal global patterns of mercury pollution and bioavailability in the world's oceans. *Pro. Natl. Acad. Sci. U.S.A*., **2021**, *118*, 1-6 ; DOI 10.1073/pnas.2111205118.

[23] Albertos, S.; Berenguer, N. I.; Sánchez-Virosta, P.; Gómez-Ramírez, P.; Jiménez, P.; Torres-Chaparro, M. Y.; Valverde, I.; Navas, I.; María-Mojica, P.; García-Fernández, A. J.; Espín, S. Mercury Exposure in Birds Linked to Marine Ecosystems in the Western Mediterranean. *Arch. Environ. Contam. Toxicol.* **2020,** *79,* 435–453 ; DOI 10.1007/s00244-020-00768-1.

[24] Gustin, M. S.; Bowman, K.; Branfireun, B.; Chetelat, J.; Eckley, C. S.; Hammerschmidt, C. R.; Lamborg, C.; Lyman, S.; Martinez-Cortizas, A.; Sommar, J.; Tsui, M. T.-K.; Zhang, T. Mercury biogeochemical cycling: A synthesis of recent scientific advances. *Sci. Total Environ*. **2020**, *737*, 139619 ; DOI 10.1016/j.scitotenv.2020.139619.

[25] *AMAP/UN Environment*. *Technical Background Report for the Global Mercury Assessment 2018*. Arctic Monitoring and Assessment Programme, Oslo, Norway/UN Environment Programme, Chemicals and Health Branch, Geneva, Switzerland. viii + 426 pp including E-Annexes. **2019**. https://www.amap.no/documents/doc/technical-background-report-for-the-global-mercury-assessment-2018/1815.

[26] Crise, A.; Allen, J. I.; Baretta, J.; Crispi, G.; Mosetti, R.; Solidoro, C. The Mediterranean pelagic ecosystem response to physical forcing. *Progr. Oceanogr*. **1999**, *44*, 219-243 ; DOI 10.1016/S0079-6611(99)00027-0.

[27] Millot, C.; Taupier-Letage, I. Circulation in the Mediterranean. In *The Mediterranean Sea;* Saliot, A. Ed.; Hdb. Env. Chem. Vol. 5, Part K, 29–66. Springer-Verlag Berlin Heidelberg 2005; pp 414; DOI 10.1007/b107143.

[28] Richon, C.; Dutay, J.-C.; Bopp, L; Le Vu, B.; Orr, J. C.; Somot, S.; Dulac, F. Biogeochemical response of the Mediterranean Sea to the transient SRES-A2 climate change scenario. *Biogeosciences* **2019***, 16*, 135-165 ; DOI 10.5194/bg-16-135-2019.

[29] Durrieu de Madron, X.; Guieu, C.; Sempéré, R.; Conan, P.; Cossa, D.; D'Ortenzio, F.; Estournel, C.; Gazeau, F.; Rabouille, C.; Stemmann, L.; Bonnet, S.; Diaz, F.; Koubbi, P.; Radakovitch, O.; Babin, M.; Baklouti, M.; Bancon-Montigny, C.; Belviso, S.; Bensoussan, N.; Bonsang, B.; Bouloubassi, I.; Brunet, C.; Cadiou, J.-F.; Carlotti, F.; Chami, M.; Charmasson, S.; Charrière, B.; Dachs, J.; Doxaran, D.; Dutay, J.-C.; Elbaz-Poulichet, F.; Eléaume, M.; Eyrolles, F.; Fernandez, C.; Fowler, S.; Francour, P.; Gaertner, J. C.; Galzin, R.; Gasparini, S.; Ghiglione, J.-F.; Gonzalez, J.-L.; Goyet, C.; Guidi, L.; Guizien, K.; Heimbürger, L.-E.; Jacquet, S. H. M.; Jeffrey, W. H.; Joux, F.; Le Hir, P.; Leblanc, K.; Lefèvre, D.; Lejeusne, C.; Lemé, R.; Loÿe-Pilot, M.-D.; Mallet, M.; Méjanelle, L.; Mélin, F.; Mellon, C.; Mérigot, B.; Merle, P.-L.; Migon, C.; Miller, W. L.; Mortier, L.; Mostajir, B.; Mousseau, L.; Moutin, T.; Para, J.; Pérez, T.; Petrenko, A.; Poggiale, J.-C.; Prieur, L.; Pujo-Pay, M.; Pulido-Villena, Raimbault; P., Rees, A. P.; Ridame, C.; Rontani, J.-F.; Ruiz Pino, D.; Sicre, M. A.; Taillandier, V.; Tamburini, C.; Tanaka, T.; Taupier-Letage, I.; Tedetti, M.; Testor, P.; Thébault, H.; Thouvenin, B.; Touratier, F.; Tronczynski, J.; Ulses, C.; Van Wambeke, F.; Vantrepotte, V.; Vaz, S.; Verney, R. Marine ecosystems' responses to climatic and anthropogenic forcings in the Mediterranean. *Prog. Oceanogr.* **2011**, *91*, 97–166 ; DOI 10.1016/j.pocean.2011.02.003.

[30] Horvat, M.; Covelli, S.; Faganelli, J.; Logar, M.; Mandic, V.; Rajar, R.; Sirca, A.; Zagar, D. Mercury in contaminated coastal environments; a case study: the Gulf of Trieste. *Sci. Total Environ.* **1999***, 237-238*, 43-56 ; DOI 10.1016/S0048-9697(99)00123-0.

[31] Covelli, S.; Langone, L.; Acquavita, A.; Piani, R.; Andrea, E. Historical flux of mercury associated with mining and industrial sources in the Marano and Grado Lagoon (northern Adriatic Sea). *Estuar. Coast Shelf Sci*. **2012**, *113*, 7–9.

[32] Canu, D. M.; Rosati, G.; Solidoro, C.; Heimbürger, L. E.; Acquavita, A. A comprehensive assessment of the mercury budget in the Marano–Grado Lagoon (Adriatic Sea) using a combined observational modeling approach. *Mar. Chem.* **2015**, *177*, 742 - 752 ; DOI 10.1016/j.marchem.2015.10.013.

[33] Rosati, G.; Solidoro, C.; Canu, D. Mercury dynamics in a changing coastal area over industrial and postindustrial phases: Lessons from the Venice Lagoon. *Sci. Total Environ*. **2020**, *743*, 1–15 ; DOI 10.1016/j.scitotenv.2020.140586.

[34] Tessier, E.; Garnier, C.; Mullot, J.-U.; Lenoble, V.; Arnaud, M.; Raynaud, M.; Mounier, S. Study of the spatial and historical distribution of sediment inorganic contamination in the Toulon bay (France). *Mar. Pollut. Bull*. **2011**, *62*, 2075-2086 ; DOI 10.1016/j.marpolbul.2011.07.022.

[35] German, C. R. C.; Casciotti, K. A.; Dutay, J.-C.; Heimbürger, L. E.; Jenkins, W. J.; Measures, C. I.; Mills, R. A.; Obata, H.; Schlitzer, R.; Tagliabue, A.; Turner, D. R.; Whitby, H. Hydrothermal impacts on trace element and isotope ocean biogeochemistry. *Phil. Trans. R. Soc*., *A Math. Phys. Eng. Sci.* **2016**, *374*, 20160035 ; DOI 10.1098/rsta.2016.0035.

[36] Bagnato, E.; Oliveri, E.; Acquavita, A.; Covelli, S.; Petranich, E.; Barra, M.; Italiano, F.; Parello, F.; Sprovieri, M. Hydrochemical mercury distribution and air-sea exchange over the submarine hydrothermal vents off-shore Panarea Island (Aeolian arc, Tyrrhenian Sea). *Mar. Chem.* **2017***, 194*, 63-78 ; DOI 10.1016/j.marchem.2017.04.003.

[37] Ferrara, R.; Mazzolai, B.; Lanzillotta, E.; Nucaro, E.; Pirrone, N. Volcanoes as emission sources of atmospheric mercury in the Mediterranean basin. *Sci. Total Environ.* **2000***, 259*, 115-121 ; DOI 10.1016/S0048-9697(00)00558-1.

[38] Edwards, B. A.; Kushner, D. S.; Outridge, P. M.; Wang, F. Fifty years of volcanic mercury emission research: Knowledge gaps and future directions. *Sci. Total Environ*. **2020**, *757*, 143800 ; DOI 10.1016/j.scitotenv.2020.143900.

[39] Cossa, D.; Martin, J.-M.; Takayanagi, K.; Sanjuan, J. The Distribution and Cycling of Mercury in the Western Mediterranean. *Deep Sea Res. II* **1997***, 44*, 721-740 *;* DOI 10.1016/S0967-0645(96)00097-5.

[40] Rajar, R.; Četina, M.; Horvat, M.; Žagar, D. Mass balance of mercury in the Mediterranean Sea. *Mar. Chem.* **2007***, 107,* 89–102 ; DOI 10.1016/j.marchem.2006.10.001.

[41] Žagar, D.; Sirnik, N.; Četina, M.; Horvat, M.; Kotnik, J.; Ogrinc, N.; Hedgecock, I. M.; Cinnirella, S.; de Simone, F.; Gencarelli, C. N.; Pirrone, N. Mercury in the Mediterranean. Part 2: processes and mass balance. *Environ. Sci. Pollut. Res.* **2014**, *21*, 4081–4094 ; DOI 10.1007/s11356-013-2055-5.

[42] Ogrinc, N.; Kotnik, J.; Fajon, V.; Monperrus, M.; Kocman, D.; Vidimova, K.; Amouroux, D.; Žižek, S.; Horvat, M. Distribution of Mercury and Methylmercury in Sediments of the Mediterranean Sea. *Mar. Chem*. **2007**, *107*, 31–48 ; DOI 10.1016/j.marchem.2007.01.019.

[43] Cossa, D.; Durrieu de Madron, X.; Schäfer, J.; Lanceleur, L.; Guédron, S.; Buscail, R.; Thomas, B.; Naudin, J.-J. The open sea as the main source of methylmercury in the water column of the Gulf of Lions (Northwestern Mediterranean margin). *Geochim. Cosmochim. Acta* **2017**, *199*, 212-231 ; DOI 10.1016/j.gca.2016.11.037.

[44] Monperrus, M.; Tessier, E.; Amouroux, D.; Leynaert, A.; Huonnic, P.; Donard, O. F. X. Mercury methylation, demethylation and reduction rates in coastal and marine surface waters of the Mediterranean Sea. *Mar. Chem*. **2007**, *107*, 49-63. DOI 10.1016/j.marchem.2007.01.018.

[45] Rosati, G.; Heimbürger, L. E.; Melaku Canu, D.; Lagane, C.; Laffont, L.; Rijkenberg, M. J. A.; Gerringa, L. J. A.; Solidoro, C.; Gencarelli, C. N.; Hedgecock, I. M.; de Baar, H. J. W.; Sonke, J. E. Mercury in the Black Sea: New insights from measurements and numerical modeling. *Global Biogeochem. Cy.* **2018**, *32* ; DOI 10.1002/2017GB005700.

[46] Cossa, D.; Knoery, J.; Boye, M.; Marusczak, N.; Thomas, B.; Courau, P.; Sprovieri, F. Oceanic mercury concentrations on both sides of the Strait of Gibraltar decreased between 1989 and 2012.

Anthropocene **2019**, *29*, 100230. Doi.org/10.1016/j.ancene.2019.100230.

[47] Fenoglio-Marc, L.; Mariotti, A.; Sannino, G.; Meyssignac, B.; Carillo, A.; Struglia, M. V.; Rixen, M. Decadal variability of net water flux at the Mediterranean Sea Gibraltar Strait. *Glob. Planet. Change* **2013**, *100*, 1-10 ; DOI 10.1016/j.gloplacha.2012.08.007.

[48] Chouvelon, T.; Cresson, P.; Bouchoucha, M.; Brach-Papa, C.; Bustamante, P.; Crochet, S.; Fabri, M.-C.; Marco-Miralles, F.; Thomas, B.; Knoery, J. Oligotrophy as a major driver of Hg bioaccumulation in marine medium- to high-trophic level consumers: an ecosystem-comparative study. *Environ. Pollut.* **2018***, 233*, 844-854 ; DOI j.envpol.2017.11.015.

[49] Wang, F.; Outridge, P. M.; Feng, X.; Meng, B.; Heimbürger-Boavida, L.-E.; Mason R. P. How closely do mercury trends in fish and other aquatic wildlife track those in the atmosphere? - Implications for evaluating the effectiveness of the Minamata Convention. *Sci. Total Environ*. **2019**, *674*, 58–70 ; DOI 10.1016/j.scitotenv.2019.04.101.

[50] Pirrone, N.; Costa, P.; Pacyna, J. M.; Ferrara, R. Mercury emissions to the atmosphere from natural and anthropogenic sources in the Mediterranean region. *Atmos. Environ*. **2001**, *35*(17), 2997-30006 ; DOI 10.1016/S1352-2310(01)00103-0.

[51] Cinnirella, S.; Pirrone, N.; Allegrini, A.; Guglietta, D. Modeling mercury emissions from forest fires in the Mediterranean region. *Environ. Fluid. Mech.* **2008**, *8***,** 129–145 ; DOI 10.1007/s10652-007-90.

[52] Sprovieri, F.; Pirrone, N.; Gardfeldt, K.; Sommar, J. Atmospheric Mercury Speciation in the Marine Boundary Layer along 6000 km Cruise path over the Mediterranean Sea. *Atmos. Environ.* **2003***, 37/S1*, 63-71 ; DOI 10.1016/S1352-2310(03)00237-1.

[53] Sprovieri, F.; Hedgecock, I. M.; Pirrone, N. An investigation of the origins of reactive gaseous mercury in the Mediterranean marine boundary layer. *Atmos. Chem. Phys*. **2010**, *10*, 3985-3997 ; DOI:10.5194/acp-10-3985-2010.

[54] Hedgecock, I. M., Pirrone, N., Sprovieri, F., Pesenti, E. 2003. Reactive Gaseous Mercury in the Marine Boundary Layer: Modeling and Experimental Evidence of its Formation in the Mediterranean. *Atmos. Environ.* **2003**, *37/S1*, 41-49 ; DOI 10.1016/S1352-2310(03)00236-X.

[55] Hedgecock, I. M.; Pirrone, N. Chasing Quicksilver: Modeling the Atmospheric Lifetime of Hg0(g) in the Marine Boundary Layer at Various Latitudes. *Environ. Sci. Technol*. **2004**, *38*, 69–76 ; DOI.org/10.1021/es034623z.

[56] Wängberg, I.; Munthe, J.; Amouroux, D.; Andersson, M. E.; Fajon, V.; Ferrara, R.; Gårdfeldt, K.; Horvat, M.; Mamane, Y.; Melamed, E.; Monperrus, M.; Ogrinc, N.; Yossef, O.; Pirrone, N.; Sommar, J.; Sprovieri, F. 2008. Atmospheric mercury at Mediterranean coastal stations. *Environ. Fluid Mech.* **2008**, *8*(2), 101-116 ; DOI 10.1007/s10652-007-9047-2.

[57] Gårdfeldt, K.; Sommar, J.; Ferrara, R.; Ceccarini, C.; Lanzillotta, E.; Munthe, J.; Wängberg, I.; Lindqvist, O.; Pirrone, N.; Sprovieri, F.; Pesenti, E.; Strömberg, D. Evasion of mercury from coastal and open waters of the Atlantic Ocean and the Mediterranean Sea. *Atmos. Environ.* **2003***, 37*, 73 - 84 ; DOI 10.1016/S1352-2310(03)00238-3.

[58] Andersson, M. E.; Gårdfeldt, K.; Wängberg, I.; Sprovieri, F.; Pirrone, N.; Lindqvist, O. Seasonal and daily variation of mercury evasion at coastal and off shore sites from the Mediterranean Sea. *Mar. Chem.* **2007,** *104*, 214 - 226 ; DOI 10.1016/j.marchem.2006.11.003.

[59] Fantozzi, L.; Manca, G.; Ammoscato, I.; Pirrone, N.; Sprovieri, F. The cycling and sea–air exchange of mercury in the waters of the Eastern Mediterranean during the 2010 MED-OCEANOR cruise campaign. *Sci. Total Environ*. **2013**, 448(15), 151-162 ; DOI 10.1016/j.scitotenv.2012.09.062.

[60] Nerentorp Mastromonaco, M. G.; Gårdfeldt, K.; Wängberg, I. Seasonal and spatial evasion of mercury from the western Mediterranean Sea. *Mar. Chem*. **2017**, *193*, 34–43 ; DOI 10.1016/j.marchem.2017.02.003, 2017b.

[61] Liss, P. S.; Slater, P. G. Flux of Gases across the Air-Sea Interface. *Nature* **1974***, 247*(5438), 181-184 ; DOI 10.1038/247181a0.

[62] Liss, P. S.; Merlivat, L. Air-Sea Gas Exchange Rates: Introduction and Synthesis. In *The Role of Air-Sea Exchange in Geochemical Cycling*; Buat-Ménard P. Ed.; NATO ASI Series (Series C: Mathematical and Physical Sciences, Vol 185). Springer, Dordrecht 1986; pp 549 ; DOI 10.1007/978-94-009-4738-2-5.

[63] Wanninkhof, R. Relationship between wind speed and gas exchange over the ocean. *J. Geophys. Res.* **1992***, 97*(C5), 7373-7382 ; DOI 10.1029/92JC00188.

[64] Wanninkhof, R.; McGillis, W. R. A cubic relationship between air-sea CO_2 exchange and wind speed. *Geophys. Res. Letters* **1999***, 26*(13), 1889-1892 ; DOI 10.1029/1999GL900363.

[65] Nightingale, P. D.; Malin, G.; Law, C. S.; Watson, A. J.; Liss, P. S.; Liddicoat, M. I.; Boutin, J.; Upstill-Goddard, R. C. In situ evaluation of air-sea gas exchange parameterizations using novel conservative and volatile tracers. *Global Biogeochem. Cy.* **2000***, 14*(1), 373-387 ; DOI 10.1029/1999GB900091.

[66] McGillis, W. R.; Edson, J. B.; Hare, J. E.; Fairall, C. W. Direct covariance air-sea CO_2 fluxes. *J. Geophys. Res. Oceans* **2001**, *106*(C8), 16729-16745 ; DOI 10.1029/2000JC000506.

[67] Johnson, M. T. A numerical scheme to calculate temperature and salinity dependent air-water transfer velocities for any gas. *Ocean Sci.* **2010**, *6*(4), 913-932 ; DOI 10.5194/os-6-913-2010.

[68] Zhang, L.; Zhou, P.; Cao, S.; Zhao, Y. Atmospheric mercury deposition over the land surfaces and the associated uncertainties in observations and simulations: a critical review. *Atmos. Chem. Phys*. **2019**, *19*, 15587-15608 ; DOI 10.5194/acp-19-15587-2019

[69] Tomazic, Š.; Ličer, M.; Žagar, D. Numerical modelling of mercury evasion in a two-layered Adriatic Sea using a coupled atmosphere-ocean model ocean model. *Mar. Pollut. Bull*. **2018**, *135*, 1164-1173 ; DOI 10.1016/j.marpolbul.2018.08.064

[70] Sharif, A.; Tessier, E.; Bouchet, S.; Monperrus, M.; Pinaly, H.; Amouroux, D. Comparison of Different Air-Water Gas Exchange Models to Determine Gaseous Mercury Evasion from Different European Coastal Lagoons and Estuaries. *Water Air Soil Pollut.* **2013***, 224*(7), 1606 ; DOI 10.1007/s11270-013-1606-1.

[71] Abril, G.; Commarieu, M.-V.; Sottolichio, A.; Bretel, P.; Guérin, F. Turbidity limits gas exchange in a large macrotidal estuary. *Estuar. Coast. Shelf Sci.* **2009***, 83*, 342-348 ; DOI 10.1016/j.ecss.2009.13.006.

[72] Bagnato, E.; Sproveri, M.; Barra, M.; Bitetto, M.; Bonsignore, M.; Calabrese, S.; Stefano, V. D.; Oliveri, E.; Parello, F.; Mazzola, S. The sea–air exchange of mercury (Hg) in the marine boundary layer of the Augusta basin (southern Italy): Concentrations and evasion flux. *Chemosphere* **2013**, *93*(9), 2024 - 2032 ; DOI 10.1016/j.chemosphere.2013.07.025.

[73] Floreani, F.; Acquavita, A.; Petranich, E.; Covelli, S. Diurnal fluxes of gaseous elemental mercury from the water-air interface in coastal environments of the northern Adriatic Sea. *Sci. Total Environ.* **2019**, *668*, 925 - 935 ; DOI 10.1016/j.scitotenv.2019.03.012.

[74] Sommar, J.; Osterwalder, S.; Zhu, W. Recent advances in understanding and measurement of Hg in the environment: Surface-atmosphere exchange of gaseous elemental mercury (Hg^0). *Sci. Total Environ.* **2020***, 721*, 137648 ; DOI 10.1016/j.scitotenv.2020.137648.

[75] Cossa, D.; Coquery, M. The Mediterranean mercury anomaly, a geochemical or a biological issue. In *The Mediterranean Sea*; Saliot, A. Ed.;. Hdb. Env. Chem. *Vol. 5*, Part K, 177-208. Springer-Verlag Berlin Heidelberg 2005; pp 414 ; DOI:10.1007/b107147.

[76] Sprovieri, F; Pirrone, N.; Bencardino, M.; D'Amore, F.; Angot, H.; Barbante, C.; Brunke, E.-G.; Arcega-Cabrera, F.; Cairns, W.; Comero, S.; del Carmen Diéguez, M.; Dommergue, A.; Ebinghaus, R.; Feng, X. B.; Fu, X.; Garcia, P. E.; Gawlik, B. M.; Hageström, U.; Hansson, K.; Horvat, M.; Kotnik, J.; Labuschagne, C.; Magand, O.; Martin, L.; Mashyanov, N.; Mkololo, T.; Munthe, J.; Obolkin, V.; Islas, M. R.; Sena, F.; Somerset, V.; Spandow, P.; Vardè1, M.; Walters, C.; Wängberg, I.; Weigelt, A.; Yang, X.; Zhang, H. Five-year records of mercury wet deposition flux at GMOS sites in the Northern and Southern hemispheres. *Atmos. Chem. Phys*. **2017**, *17*, 2689–2708 ; DOI 10.5194/acp-17-2689-2017.

[77] Gencarelli, C. N.; De Simone, F.; Hedgecock, I. M.; Sprovieri, F.; Pirrone, N. Development and application of a regional-scale atmospheric mercury model based on WRF/Chem: a Mediterranean area investigation. *Environ. Sci. Pollut. Res. Int.* **2014,** *21*(6), 4095-109 ; DOI 10.1007/s11356-013-2162-3.

[78] Gencarelli, C. N.; De Simone, F.; Hedgecock, I. M.; Sprovieri, F.; Yang, X.; Pirrone, N. European and Mediterranean mercury modelling: local and long-range contributions to the deposition flux. *Atmos. Environ*. **2015**, *117*, 162-168, PII: S1352-2310(15)30214-4 ; DOI 10.1016/j.atmosenv.2015.07.015.

[79] De Simone, F. D.; Gencarelli, C. N.; Hedgecock, I. M.; Pirrone, N. 2016. A Modeling Comparison of Mercury Deposition from Current Anthropogenic Mercury Emission Inventorie. *Environ. Sci. Technol.* **2016**, *50*(10), 5154-5162 ; DOI 10.1021/acs.est.6b00691.

[80] De Simone, F.; D'Amore, F.; Marasco, F.; Carbone, F.; Bencardino, M.; Hedgecock, I.M.; Cinnirella, S.; Sprovieri, F.; Pirrone, N. A Chemical Transport Model Emulator for the Interactive Evaluation of Mercury Emission Reduction Scenarios. *Atmosphere* **2020**, *11*, 878 ; DOI 10.3390/atmos11080878.

[81] Horowitz, H. M.; Jacob, D. J.; Zhang, Y.; Dibble, T. S.; Slemr, F.; Amos, H. M.; Schmidt, J. A.; Corbitt, E. S.; Marais, E. A.; Sunderland, E. M. A new mechanism for atmospheric mercury redox chemistry: implications for the global mercury budget. *Atmos. Chem. Phys.* **2017**, *17*(10), 6353-6371 ; DOI 10.5194/acp-17-6353-2017.

[82] Saiz-Lopez, A.; Acuña, A. U.; Trabelsi, T.; Carmona-García, J.; Dávalos, J. Z.; Rivero, D.; Cuevas, C. A.; Kinnison, D. E.; Sitkiewicz, S. P.; Roca-Sanjuán, D.; Francisco, J. S. Gas-Phase Photolysis of Hg(I) Radical Species: A New Atmospheric Mercury Reduction Process. *J. Am. Chem. Soc.* **2019***, 141*, 8698-702 ; DOI 10.1021/jacs.9b02890.

[83] Yang, X.; Jiskra, M.; Sonke, J.E. Experimental rainwater divalent mercury speciation and photoreduction rates in the presence of halides and organic carbon. *Sci. Total Environ.* **2019***, 697*, 133821 ; DOI 10.1016/j.scitotenv.2019.133821.

[84] Francés-Monerris, A.; Carmona-García, J.; Acuña, A. U.; Dávalos, J. Z.; Cuevas, C. A.; Kinnison, D. E.; Francisco, J. S.; Saiz-Lopez, A.; Roca-Sanjuán, D. Photodissociation Mechanisms of Major Mercury(II) Species in the Atmospheric Chemical Cycle of Mercury. *Angew. Chem. Int. Ed.* **2020**, *59*(19), 7605-7610 ; DOI 10.1002/anie.201915656.

[85] Jiskra, M.; Heimbürger-Boavida, L. E.; Desgranges, M. M.; Petrova, M. V.; Dufour, A.; Ferreira-Araujo, B.; Masbou, J.; Chmeleff, J.; Thyssen, M.; Point, D.; Sonke, J. E. Mercury stable isotopes constrain atmospheric sources to the ocean. *Nature* **2021**, *597***,** 678–682 ; DOI 10.1038/s41586-021-03859-8.

[86] Cossa, D.; Durrieu de Madron, X.; Schäfer, J.; Guédron, S.; Marusczak, N.; Castelle, S.; Naudin, J.-J. Sources and exchanges of mercury in the waters of the Northwestern Mediterranean margin. *Progr. Oceanogr.* **2018***, 163*, 172-183 ; DOI 10.1016/j.pocean.2017.05.002.

[87] Tagliabu, A. *Elemental Distribution: Overview;* Encyclopedia of Ocean Sciences, 3rd edition; 2018 ; DOI 10.1016/B978-0-12-409548-9.10774-2.

[88] Kotnik, J.; Horvat, M.; Ogrinc, N.; Fajon, V.; Žagar, D.; Cossa, D.; Sprovieri, F.; Pirrone, N. Mercury speciation in the Adriatic Sea. *Mar. Pollut. Bull*. **2015**, *96*, 136–148 ; DOI 10.1016/j.marpolbul.2015.05.037.

[89] Heimbürger-Boavida, L. E. Mediterranean Institute of Oceanography, Université Aix-Marseille, France, unpublished results from PEACETIME cruise.

[90] Knoery, J. Ifremer, Centre Atlantique, France. Unpublished results from FENICE-GMOS cruise.

[91] Heimbürger, L.-E.; D. Cossa, D.; Marty, J.-C.; Migon, C.; Averty, B.; Dufour, A.; Ras, J. 2010. Methyl mercury distributions in relation to the presence of nano and picophytoplankton in an oceanic water column (Ligurian Sea, North-western Mediterranean). *Geochim. Cosmochim. Acta* **2010**, *74*, 5549-4459 ; DOI.org:10.1016/j.gca.2010.06.036.

[92] Sunderland, E. M.; Krabbenhoft, D. P.; Moreau, J. W.; Strode, S. A.; Landing, W. M. Mercury sources, distribution, and bioavailability in the North Pacific Ocean: Insights from data and models. *Global Biogeochem. Cy.* **2009**, *23*(2), 14 p ; DOI 10.1029/2008gb003425

[93] Munson, K. M.; Lamborg, C. H.; Swarr, G. J., Saito, M. A. Mercury species concentrations and fluxes in the Central Tropical Pacific Ocean. *Global Biogeochem. Cy.* **2015***, 29* ; DOI 10.1002/2015GB005120.

[94] Cossa, D.; Heimbürger, L. E.; Lannuzel, D.; Rintoul, S. R.; Butler, E. C. V.; Bowie, A. R.; Averty, B.; Watson, R. J.; Remenyi, T. Mercury in the Southern Ocean. *Geochim. Cosmochim. Acta* **2011***, 75*, 4037–4052 ; DOI 10.1016/j.gca.2011.05.001.

[95] Heimbürger-Boavida, L.E. Mediterranean Institute of Oceanography, Université Aix-Marseille, France. unpublished results from GEOVIDE-GEOTRACES cruise.

[96] Mason, R. P.; Fitzgerald, W. F. Alkylmercury species in the equatorial Pacific. *Nature* **1990**, *347*(6292), 457-459 ; DOI 10.1038/347457a0.

[97] Cossa, D.; Averty, B.; Pirrone, N. The origin of methylmercury in open Mediterranean waters. *Limnol. Oceanogr.* **2009**, *54*, 837-844 ; DOI 10.4319/lo.2009.54.3.0837.

[98] Blum, J. D.; Popp, B. N.; Drazen, J. C.; Choy, C. A.; Johnson, M. W. Methylmercury production below the mixed layer in the North Pacific Ocean. *Nat. Geosci.* **2013**, *6*, 879-884 ; DOI 10.1038/NGEO1918.

[99] Kotnik, J.; Sprovieri, F.; Ogrinc, N.; Horvat, M.; Pirrone, N. Mercury in the Mediterranean, part I: spatial and temporal trends. *Environ. Sci. Pollut. Res.* **2014**, *21*, 4063-4080 ; DOI 10.1007/s11356-013-2378-2.

[100] Gascon Diez, E.; Loizeau, J.-L.; Cosio, C.; Bouchet, S.; Adatte, T.; Amouroux D., Bravo, A. Role of Settling Particles on Mercury Methylation in the Oxic Water Column of Freshwater Systems. *Environ. Sci. Technol*. **2016**, *50*, 11672-11679 ; DOI 10.1021/acs.est.6b03260.

[101] Munson, K. M.; Lamborg, C. H.; Boiteau, R. M.; Saito, M. A. Dynamic mercury methylation and demethylation in oligotrophic marine water. *Biogeosciences* **2018***, 15*, 6451–6460 ; DOI 10.5194/bg-15-6451-2018.

[102] Rizzo, A. L.; Caracausi, A.; Chavagnac, V.; Nomikou, P.; Polymenakou, P. N.; Mandalakis, M.; Kotoulas, G.; Magoulas, A.; Castillo, A.; Lampridou, D.; Marusczak, N.; Sonke J. E. Geochemistry of CO_2-Rich Gases Venting from Submarine Volcanism: The Case of Kolumbo (Hellenic Volcanic Arc, Greece). *Front. Earth Sci*. **2019**, *7*, 60 ; DOI 10.3389/feart.2019.00060.

[103] Heimbürger, L. E.; Cossa, D.; Thibodeau, B.; Khripounoff, A.; Mas, V.; Chiffoleau, J.-F.; Schmidt, S.; Migon, C. Natural and anthropogenic trace metals in sediments of the Ligurian Sea (Northwestern Mediterranean). *Chem. Geol.* **2012**, *291***,** 141–151 ; DOI 10.1016/j.chemgeo.2011.10.011.

[104] Ogrinc, N.; Hintelmann, H.; Kotnik, J.; Horvat, M.; Pirrone, N. Sources of mercury in deep-sea sediments of the Mediterranean Sea as revealed by mercury stable isotopes. *Sci. Rep.* **2019***, 9*, 11626 ; DOI 10.1038/s41598-019-48061-z.

[105] Cossa, D.; Mucci, A.; Guédron, S.; Coquery, M.; Radakovitch, O.; Escoube, R.; Campillo, S.; Heussner, S. Mercury accumulation in the sediment of the Western Mediterranean abyssal plain: A reliable archive of the late Holocene. *Geochim. Cosmochim. Acta*, **309**, 1-15 ; DOI 10.1016/j.gca.2021.06.014.

[106] Coquery, M. INRAE, Lyon, France. Unpublished results from ADIOS project.

[107] *ADIOS Final Report. Atmospheric deposition and Impact of Pollutants, key elements, and nutrients on the open Mediterranean Sea*. Section 6: detailed report related to overall project duration; 2004; pp 93; European Communities; Contract number: EVK3-CT-2000-00035 Coordinator: S. Heussner (CNRS, France); www.Cordis.europa.eu/project/id/EVK3-CT-2000-00035/results.

[108] Živković, I.; Kotnik, J.; Šolić, M.; Horvat, M. The abundance, distribution and speciation of mercury in waters and sediments of the Adriatic Sea – a review. *Acta Adriat*. **2017**, *58*, 165-186.

[109] Durrieu de Madron, X.; Wiberg, P. L.; Puig, P. Sediment dynamics in the Gulf of Lions: The impact of Extreme events. Introduction. *Cont. Shelf Res*. **2008**, *28*, 1967-1876 ; DOI 10.1016/j.csr.2008.08.001.

[110] Cossa, D.; Heimbürger, L.-E.; Pérez, F. F.; García-Ibáñez, M. I.; Sonke, J. E.; Planquette, H.; Lherminier, P.; Boutorh, J.; Cheize, M.; Menzel Barraqueta, J. L.; Shelley R.; Sarthou, G. Mercury distribution and transport in the North Atlantic Ocean along the Geotraces-GA01 transect. *Biogeosciences* **2018**, *15*(8), 2309-2323 ; DOI:10.5194/bg-15-2309-2018.

[111] Migon, C.; Heimbürger-Boavida, L.-E.; Dufour, A.; Chiffoleau, J.-F.; Cossa D. Temporal variability of dissolved trace metals at the DYFAMED time-series station, Northwestern Mediterranean. *Mar. Chem.* **2020***, 225*, 103846 *; DOI* 10.1016/j.marchem.2020.103846.

[112] Huertas, I. E.; A. F. Ríos, A. F.; García-Lafuente, J.; Navarro, G.; Makaoui, A.; Sánchez-Román, A.; Rodriguez-Galvez, S.; Orbi, A.; Ruíz, J.; Pérez, F. F. Atlantic forcing of the Mediterranean oligotrophy, *Global Biogeochem. Cy.* **2012**, *26*, GB2022 ; DOI 10.1029/2011GB004167.

[113] Castagna, J.; Bencardino, M.; d'Amore, F.; Esposito, G.; Pirrone, N.; Sprovieri, F. Atmospheric mercury species measurements across the Western Mediterranean region: Behaviour and variability

during a 2015 research cruise campaign. *Atmos. Environ*. **2018**, *173*, 108–126 ; DOI 10.1016/j.atmosenv.2017.10.045.

[114] Bagnato, E.; Aiuppa, A.; Parello, F.; Allard, P.; Liuzzo, M.; Giudice, G.; Shinohara, H. New clues on mercury contribution from Earth volcanism. *Bull. Volcanol*. **2011**, *73*, 497-510.

[115] Bagnato, E.; Aiuppa, A.; Parello, F.; Calabrese, S.; D'Alessandro, W.; Mather, T. A.; McGonigle, A. J. S.; Pyle, D. M.; Wängberg, I., 2007. Degassing of gaseous (elemental and reactive) and particulate mercury from Mount Etna volcano (Southern Italy). *Atmos. Environ*. **2007**, *41*, 7377–7388 ; DOI 10.1016/j.atmosenv.2007.05.060.

[116] Bagnato, E.; Tamburello, G.; Avard, G.; Martinez-Cruz, M.; Enrico, M.; Fu, X.; Sprovieri, M.; Sonke, J. E. Mercury Fluxes from Volcanic and Geothermal Sources: An Update. *Geol. Soc. Lond. Spec. Publ.* **2015**, *410*, 263–285 ; DOI 10.1144/SP410.2.

[117] Carn, S. A.; Fioletov, V. E.; McLinden, C. A.; Li, C.; Krotkov, N. A. A. Decade of Global Volcanic SO_2 Emissions Measured from Space. *Sci. Rep.* **2017**, *7*, 44095 ; DOI.org/10.1038/srep44095.

[118] Bowman, K. L.; Hammerschmidt, C. R.; Lamborg, C. H.; Swarr, G. Mercury in the North Atlantic Ocean: the U.S. GEOTRACES zonal and meridional sections. *Deep-Sea Res*. *II* **2015**, *116*, 251–261.

[119] Bratkič, A.; M. Vahčič, M.; Kotnik, J.; Obu Vazner, K.; Begu, E.; Woodward, E. M. S. Horvat, M. Mercury presence and speciation in the South Atlantic Ocean along the 40°S transect, *Global Biogeochem. Cy.* **2016**, *30*, 105–119 ; DOI 10.1002/2015GB005275.

[120] Panagos, P.; Jiskra, M.; Borrelli, P.; Liakos, L.; Ballabio, C. Mercury in European topsoils: Anthropogenic sources, stocks and fluxes. *Environ. Res*. **2021**, 201, 111556 ; DOI 10.1016/j.envres.2021.111556.

[121] Bouraoui, F.; Grizzetti, B.; Aloe, A. Estimation of water fluxes into the Mediterranean Sea. *J. Geophys. Res*. **2010**, *115*, D21116 ; DOI:10.1029/2009JD013451.

[122] Shaltout, M.; Omstedt, A. Calculating the water and heat balances of the Eastern Mediterranean Basin using ocean modelling and available meteorological, hydrological and ocean data. *Oceanologia* **2012**, *54*, 199-232 ; DOI:10.597/oc.54-2.199.

[123] Shaltout, M.; Omstedt, A. Modelling the water and heat balances of the Mediterranean Sea using a two-basin model and available meteorological, hydrological, and ocean data. *Oceanologia* **2015**, *57,* 116-131 ; DOI 10.1016/j.oceano.2014.11.001.

[124] Petrova, M. V. Mediterranean Institute of Oceanography, Université Aix-Marseille, France

[125] Trezzi, G.; Garcia-Orellana, J.; Rodellas, V.; Santos-Echeandia, J.; Tovar-Sánchez, A.; Garcia-Solsona, E.; Masqué, P. Submarine groundwater discharge: A significant source of dissolved trace metals to the North Western Mediterranean Sea. *Mar. Chem.* **2016**, *186*, 90-100.

[126] Salvagio Manta, D.; Bonsignore, M.; Oliveri, E.; Barra, M.; Tranchida, G.; Giaramita, L.; Mazzola, S.; Sprovieri, M. Fluxes and the mass balance of mercury in Augusta Bay (Sicily, southern Italy). *Estuar. Coast. Shelf Sci*. **2016**, *181*, 134–143 ; DOI 10.1016/j.ecss.2016.08.01.

[127] Eakins, B. W.; Sharman, G. F. *Volumes of the World's Oceans from ETOPO1*, NOAA National Geophysical Data Center, Boulder, CO, 2010; www.ngdc.noaa.gov/mgg/global/etopo1_ocean_volumes.html.

[128] Gilmour, C. C.; Podar, M.; Bullock, A. L.; Graham, A. M.; Brown, S. D.; Somenahally, A. C.; Johs, A.; Hurt, R. A.; Bailey, K. L.; Elias, D. A. Mercury methylation by novel microorganisms from new environments. *Environ. Sci. Technol*. **2013**, *47*, 11810–11820 ; DOI 10.1021/es403075t.

[129] Parks, J. M.; Johs, A.; Podar, M.; Bridou, R.; Hurt, R. A.; Smith, S. D.; Tomanicek, S. J.; Qian, Y.; Brown, S. D.; Brandt, C. C.; Palumbo, A. V; Smith, J. C.; Wall, J. D.; Elias, D. A.; Liang, L. The genetic basis for bacterial mercury methylation. *Science* **2013**, *339*, 1332–1335 ; DOI 10.1126/science.1230667.

[130] Podar, M.; Gilmour, C. C.; Brandt, C. C.; Soren, A.; Brown, S. D.; Crable, B. R.; Palumbo, A. V.; Somenahally, A. C.; Elias, D. A. Global prevalence and distribution of genes and microorganisms involved in mercury methylation. *Sci. Adv.* **2015***, 1*, e1500675–e1500675 ; DOI 10.1126/sciadv.1500675.

[131] Gionfriddo, C. M.; Tate, M. T.; Wick, R. R.; Schultz, M. B.; Zemla, A.; Thelen, M. P.; Schofield, R.; Krabbenhoft, D. P.; Holt, K. E.; Moreau, J. W. Microbial mercury methylation in Antarctic sea ice.

Nat. Microbiol. **2016***, 1*, 16127 ; DOI 10.1038/nmicrobiol.2016.127.

[132] Villar, E.; Cabrol, L.; Heimbürger-Boavida, L.-E. Widespread microbial mercury methylation genes in the global ocean. *Environ. Microbiol. Rep*. **2020**, *12*(3), 277-287 ; DOI 10.1111/1758-2229.12829.

[133] Mason, R. P.; Lawson, N. M.; Sheu, G. Mercury in the Atlantic Ocean: factors controlling air – sea exchange of mercury and its distribution in the upper waters. *Deep Sea Res. Part II* **2001**, *48*, 2829–2853 ; DOI 10.1016/S0967-0645(01)00020-0.

[134] Barkay, T.; Miller, S. M.; Summers, A. O. 2003. Bacterial mercury resistance from atoms to ecosystems. *FEMS Microbiol. Rev.* **2003**, *27*, 355–384 ; DOI 10.1016/S0168-6445(03)00046-9.

[135] Zhang, T.; Hsu-kim, H. Photolytic degradation of methylmercury enhanced by binding to natural organic ligands. *Nat. Geosci.* **2010***, 3*, 473–476 ; DOI 10.1038/ngeo892.

[136] Costa, M.; Liss, P. S. Photoreduction of mercury in sea water and its possible implications for Hg 0 air–sea fluxes. *Mar. Chem.* **1999**, *68*, 87–95 ; DOI 10.1016/S0304-4203(99)00067-5.

[137] Qureshi, A.; O'Driscoll, N. J.; Macleod, M.; Neuhold, Y. M.; Hungerbühler, K. Photoreactions of mercury in surface ocean water: Gross reaction kinetics and possible pathways. *Environ. Sci. Technol*. **2010**, *44,* 644–649 ; DOI 10.1021/es9012728

[138] Black, F. J.; Poulin, B. A.; Flegal, A. R. Factors controlling the abiotic photo-degradation of monomethylmercury in surface waters. *Geochim. Cosmochim. Acta* **2012**, *84*, 492–507. DOI 10.1016/j.gca.2012.01.019.

[139] Marvin-Dipasquale, M.; Agee, J.; McGowan, C.; Oremland, R. S.; Thomas, M.; Krabbenhoft, D.; Gilmour, C. Methyl-Mercury Degradation Pathways: A Comparison among Three Mercury-Impacted Ecosystems. *Environ. Sci. Technol*. **2000**, *34*, 4908-4916 ; DOI 10.1021/es0013125.

[140] Bowman, K. L.; Collins, R. E.; Agather, A.M.; Lamborg, C. H.; Hammerschmidt, C. R.; Kaul, D.; Dupont, C. L.; Christensen, G. A.; Elias, D. A. Distribution of mercury-cycling genes in the Arctic and equatorial Pacific Oceans and their relationship to mercury speciation. *Limnol. Oceanogr.* **2020**, *65*, S310–S320 ; DOI 10.1002/lno.11310.

[141] Baya, P. A.; Gosselin M.; Lehnherr I.; St. Louis V. L.; Hintelmann, H. Determination of monomethylmercury and dimethylmercury in the arctic marine boundary layer. *Environ. Sci. Technol*. **2015**, *49*, 223-232 ; DOI 10.1021/es502601z.

[142] Jonsson, S.; Mazrui, N. M.; Mason, R. P. Dimethylmercury Formation Mediated by Inorganic and Organic Reduced Sulfur Surfaces. *Sci. Rep.* **2016**, *6*, 27958 ; DOI 10.1038/srep27958.

[143] Storelli, M.; Marcotrigiano, G. Total mercury levels in muscle tissue of swordfish (*Xiphias gladius*) and bluefin tuna (*Thunnus thynnus*) from the Mediterranean sea (Italy). *Food. Prot*. **2001**, *64*, 1058-1061.

[144] Storelli, M.; Giacominelli-Stuffler, R. ; Storelli, A. ; Marcotrigiano, G. Accumulation of mercury, cadmium, lead and arsenic in swordfish and bluefin tuna from Mediterranean Sea : a comparative study. *Mar. Pollut. Bull*. **2005**, *50*, 1004-1007.

[145] Abolghait S. K.; Garbaj A. M. Determination of cadmium, lead and mercury residual levels in meat of canned light tuna (*Katsuwonus pelamis* and *Thunnus albacares*) and fresh little tunny (*Euthynnus alletteratus*) in Libya. *Open Vet. J.* **2015***, 5*, 130-137.

[146] Annibaldi, A.; Truzzi, C.; Carnevali, O.; Pignalosa, P.; Api, M.; Scarponi, G.; Silvia Illuminati S. 2019. Determination of Hg in farmed and wild Atlantic Bluefin tuna (*Thunnus thynnus* L.) muscle. *Molecules* **2019***, 24*(7), 1273. DOI 10.3390/molecules24071273.

[147] Barone, G.; Dambrosio, A.; Storelli, A.; Garofalo, R.; Busco, V. P.; Storelli M. M. 2018. Estimated Dietary Intake of Trace Metals from Swordfish Consumption: A Human Health Problem. *Toxics* **2018,** *6*, 22. DOI 10.3390/toxics6020022.

[148] Cinnirella, S.; Bruno, D. E.; Pirrone, N.; Horvat, M.; Živković, I.; Evers, D. C.; Johnson, S.; Sunderland, E. M. Mercury concentrations in biota in the Mediterranean Sea, a compilation of 40 years of surveys. *Sci. Data* **2019**, *6*, 205 ; DOI 10.1038/s41597-019-0219-y.

[149] Esposito, M.; De Roma, A.; La Nuera, R.; Picazio, G.; Gallo, P. Total mercury content in commercial swordfish (*Xiphias gladius*) from different FAO fishing areas. *Chemosphere* **2018**, *197*, 14-19 ; DOI 10.1016/j.chemoshere.2018.01.015.

[150] Lee, C. S.; Fisher, N. S. Bioaccumulation of methylmercury in a marine copepod. *Environ. Toxicol. Chem.* **2016**, *9999*, 1-7 ; DOI 10.1002/etc.3660.

[151] Mason, R. P.; Reinfelder, J. R.; Morel, F. M. F. Uptake, Toxicity, and Trophic Transfer of Mercury in a Coastal Diatom Uptake, Toxicity, and Trophic Transfer of Mercury in a Coastal Diatom. *Environ. Sci. Technol.* **1996**, *30*, 1835-1845 ; DOI 10.1021/es950373d.

[152] Lee, C. S.; Fisher, N. S. Bioaccumulation of methylmercury in a marine diatom and the influence of dissolved organic matter. *Mar. Chem.* **2017**, *197*, 70-79 ; DOI 10.1016/j.marchem.2017.09.005.

[153] Harding, G.; Dalziel, J.; Vass, P. Bioaccumulation of methylmercury within the marine food web of the outer Bay of Fundy, Gulf of Maine. *PLoS ONE* **2018***, 13*, e0197220 ; DOI 10.1371/journal.pone.0197220.

[154] Hunt, B. P. V.; Carlotti, F.; Donoso, K.; Pagano, M.; D'Ortenzio, F.; Taillandier, V.; Conan, P. Trophic pathways of phytoplankton size classes through the zooplankton food web over the spring transition period in the north-west Mediterranean Sea. *J. Geophys. Res. Oceans* **2017**, *122*, 6309-6324 ; DOI:10.1002/2016JC012658.

[155] Barbieux, M.; Uitz, J.; Gentili, B.; Pasqueron de Fommervault, O.; Mignot, A.; Poteau, A.; Schmechtig, C.; Taillandier, V.; Leymarie, E.; Penkerc'h, C.; D'Ortenzio, F.; Claustre, H.; Bricaud, A. Bio-optical characterization of subsurface chlorophyll maxima in the Mediterranean Sea from a Biogeochemical-Argo float database. *Biogeosciences* **2019**, *16*, 1321-1342 ; DOI 10.5194/bg-16-1321-2019.

[156] Harmelin-Vivien, M.; Cossa, D.; Crochet, S.; Banaru, D.; Letourneur, Y.; Mellon-Duval, C. Difference of mercury bioaccumulation in red mullets from the north-western Mediterranean and Black seas. *Mar. Pollut. Bull.* **2009**, *58*, 679-685 ; DOI 10.1016/j.marpolbul.2009.01.004.

[157] Chouvelon, T.; Strady, E.; Harmelin-Vivien, M.; Radakovitch, O.; Brach-Papa, C.; Crochet, S.; Knoery, J.; Rozuel, E.; Thomas, B.; Tronczynski, J.; Chiffoleau, J.-F. Patterns of trace metal bioaccuumulation and trophic transfer in a phytoplankton-zooplankton-small pelagic fish marine food web. *Mar. Pollut. Bull.* **2019**, *146*, 1013-1030 ; DOI 10.1016/j.marpolbul.2019.07.047.

[158] Zhang, Y.; Soerensen, A. L.; Schartup, A. T.; Sunderland, E. M. A global model for methylmercury formation and uptake at the base of marine food webs. *Global Biogeochem. Cy.* **2020***, 34*, e2019GB006348 ; DOI 10.1029/2019GB006348.

[159] Twining, B. S.; Fisher, N. S. Trophic transfer of trace metals from protozoa to mesozooplankton. *Limnol. Oceanogr.* **2004**, *49*, 2004, 28–39.

[160] Fisk, A. T.; Hobson, K. A.; Norstrom, R. J. Influence of chemical and biological factors on trophic transfer of persistent organic pollutants in the Northwater Polynia marine food web. *Environ. Sci. Technol.* **2001**, *35*, 732–738 ; DOI 10.1021/es001459w.

[161] Mathews, T.; Fisher N. S. Dominance of dietary intake of metals in marine elasmobranch and teleost fish. *Sci. Tot. Environ.* **2009**, *407*, 5156–5161 ; DOI 10.1016/j.scitotenv.2009. 06.003.

[162] Joiris, C. R.; Holsbeek, L.; Laroussi Moatemri, N. Total and methylmercury in sardines *Sardinella aurita* and *Sardina pilchardus* from Tunisia. *Mar. Pollut. Bull*. **1999**, *38*, 188-192 ; DOI.org/10.1016/S0025-326X(98)00171-4.

[163] Stacy, W. L.; Lepak, J. M. Relative influence of prey mercury concentration, prey energy density and predator sex on sport fish mercury concentrations. *Sci. Total Environ*. **2012**, *437*, 104-109 ; DOI 10.1016/j.scitotenv.2012.07.064.

[164] Pinzone, M.; Damseaux, F.; Michel, L. N.; Das, K. Stable isotope ratios of carbon, nitrogen and sulphur and mercury concentrations as descriptors of trophic ecology and contamination sources of Mediterranean whales. *Chemosphere* **2019***, 237*, 124448 ; DOI 10.1016/j.chemosphere.2019.124448.

[165] Costantini, D.; Bustamante, P.; Brault-Favrou, M.; Dell'Omo, G. Patterns of mercury exposure and relationships with isotopes and markers of oxidative status in chicks of a Mediterranean seabird. *Environ. Pollut.* **2020**, *260*, 114095 ; DOI 10.1016/j.envpol.2020.114095.

[166] Bouchoucha, M.; Chekri, R.; Leufroy, A.; Jitaru, P.; Millour, S.; Marchond, N.; Chafrey, C.; Testu, C.; Zinck, J.; Cresson, P.; Mirallès, F.; Mahe, A.; Arnich, N.; Sanaa, M.; Bemrah, N.; Guérin, T. Trace

element contamination in fish impacted by bauxite red mud disposal in the Cassidaigne canyon (NW French Mediterranean). *Sci. Total Environ*. **2019**, *690*, 16-26 ; DOI 10.1016/j.stotenv.2019.06.474.

[167] Maulvault, A. L.; Custódio, A.; Anacleto, P.; Repolho, T.; Pousão, P.; Nunes, M. L.; Diniz, M.; Rosa, R.; Marques, A. Bioaccumulation and elimination of mercury in juvenile seabass (*Dicentrarchus labrax*) in a warmer environment. *Environ. Res*. **2016**, *149*, 77-85 ; DOI 10.1016/j.envres.2016.04.035.

[168] Sánchez-Muros, M. J.; Morote, E.; Gil, C.; Ramos-Miras Torrijos, M.; Rodríguez Martin, J. A. Mercury contents in relation to biometrics and proximal composition and nutritional levels of fish eaten from the Western Mediterranean Sea (Almería bay). *Mar. Pollut. Bull*. **2018**, *135*, 783-789 ; DOI 10.1016/j.marpolbul.2018.08.003.

[169] Branco, V.; Vale, C.; Canário, J.; Neves dos Santos, M. Mercury and selenium in blue shark (*Prionace glauca*, L. 1758) and swordfish (*Xiphias gladius*, L. 1758) from two areas of the Atlantic Ocean. *Environ. Pollut.* **2007**, *150*, 373-380 ; DOI 10.1016/j.envpol.2007.01.040.

[170] Cresson, P.; Bouchoucha, M.; Morat, F.; Miralles, F.; Chavanon, F.; Loizeau, V.; Cossa, D. A multitracer approach to assess the spatial contamination pattern of hake (*Merluccius merluccius*) in the French Mediterranean. *Sci. Total Environ*. **2015**, *532*, 184-194 ; DOI 10.1016/j.scitotenv.2015.06.020.

[171] Harmelin-Vivien, M.; Bodiguel, X.; Charmasson, S.; Loizeau, V.; Mellon-Duval, C.; Tronczyński, J.; Cossa, D. Differential biomagnification of PCB, PBDE, Hg and Radiocesium in the food web of the European hake from the NW Mediterranean. *Mar. Pollut. Bull.* **2012***, 64*, 974-983 ; DOI 10.1016/j.marpolbul.2012.02.014.

[172] Capelli, R.; Drava G.; Siccardi C.; De Pellegrini R.; Minganti V., 2004. Study of the distribution of trace elements in six species of marine organisms of the Ligurian Sea (North-Western Mediterranean). Comparison with previous findings. *Annali di Chimica* **2004**, *94*, 533-546 ; DOI 10.1002/adic.200490067.

[173] Cresson, P.; Fabri, M.-C.; Bouchoucha, M.; Brach Papa, C.; Chavanon, F.; Jadaud, A.; Knoery, J.; Miralles, F.; Cossa D. Mercury in organisms from the Northwestern Mediterranean slope: importance of food sources. *Sci. Total Environ*. **2014**, *497-498*, 229-238 ; DOI 10.1016/j.scitotenv.2014.07.069.

[174] Storelli, M. M.; Storelli, A.; Giacominelli-Stuffler, R.; Marcotrigiano, G. O. Mercury speciation in the muscle of two commercially important fish, hake (*Merluccius merluccius*) and striped mullet (*Mullus barbatus*) from the Mediterranean Sea: estimated weekly intake. *Food Chem.* **2005**, *89*, 295-300 ; DOI 10.1016/j.foodchem.2004.02.036.

[175] Signa, G.; Mazzola, A.; Tramati, C. D.; Vizzini, S. Diet and habitat use influence Hg and Cd transfer to fish and consequent biomagnification in a highly contaminated area: Augusta Bay (Mediterranean Sea). *Environ. Pollut*. **2017**, *230*, 394-404 ; DOI 10.1016/j.envpol.2017.06.027.

[176] Grgec, A. S.; Kljaković-Gašpić, Z.; Orct, T.; Tičina, V.; Sekovanić, A.; Jurasović, J.; Piasek, M. Mercury and selenium in fish from the eastern part of the Adriatic Sea: A risk-benefit assessment in vulnerable population groups. *Chemosphere* **2020***, 261*, 127742 ; DOI 10.1016/j.chemosphere.2020.127742.

[177] Ourgaud, M. Influence des apports anthropiques sur les flux de carbone et de contaminants dans les réseaux trophiques de 'poissons' de l'écosystème à Posidonia oceanica. Ph. D. Dissertation, Aix-Marseille University, France ; 2015 pp 350 ; www.theses.fr/2015AIXM4097.

[178] Ourgaud, M.; Ruitton, S.; Bourgogne, H.; Bustamante, P.; Churlaud, C.; Guillou, G.; Lebreton, B.; Harmelin-Vivien, M. Trace elements in a Mediterranean scorpaenid fish: bioaccumulation processes and spatial variations. *Progr. Oceanogr.* **2018***, 163*, 184-195 ; DOI 10.1016/j.pocean.2017.11.008.

[179] Chouvelon, T.; Spitz, J.; Caurant, F.; Mendez-Fernandez, P.; Autier, J.; Lassus-Debat, A.; Bustamante, P. Enhanced bioaccumulation of mercury in deep-sea fauna from the Bay of Biscay (North-East Atlantic) in relation to trophic positions identified by analysis of carbon and nitrogen stable isotopes. *Deep-Sea Res*. *I* **2012**, *65*, 113-124 ; DOI 10.1016/j.dsr.2012.02.010.

[180] Cransveld, A.; Amouroux, D.; Tessier, E.; Koutrakis, E.; Ozturk, A. A.; Bettoso, N.; Mieiro, C. L.; Bérail, S.; Barre, J. P. G.; Sturaro, N.; Schnitzler, J.; Das K. Mercury stable isotopes discriminate different populations of European seabass and trace potential Hg sources around Europe. *Environ. Sci. Technol.* **2017**, *51*, 12219-12228 ; DOI 10.1021/acs.est.7b01307.

[181] Buckman, K. L.; Lane, O.; Kotnik, J.; Bratkic, A.; Sprovieri, F.; Horvat, M.; Pirrone, N.; Evers, D. C.; Chen, C. Y. Spatial and taxonomic variation of mercury concentration in low trophic level fauna from the Mediterranean Sea. *Ecotoxicology* **2018**, *27*, 1341-1352 ; DOI 10.1007/s10646-018-1986-5.

[182] Orani, A. M.; Vassileva, E.; Azemard, S.; Thomas, O. P. Comparative study on Hg bioaccumulation and biotransformation in Mediterranean and Atlantic sponge species. *Chemosphere* **2020**, *260*, 127515 ; DOI 10.1016/j.chemosphere.2020.127515.

[183] Kucuksezgin, F.; Altay, O.; Uluturhan, E.; Kontas, A. Trace metal and organochlorine residue levels in red mullet (*Mullus barbatus*) from the Eastern Aegean, Turkey. *Wat. Res*. **2001**, *35*, 2327-2332 ; DOI 10.1016/S0043-1354(00)00504-2.

[184] Briant, N.; Chouvelon, T.; Martinez, L.; Brach-Papa, C.; Chiffoleau, J.-F.; Savoye, N.; Sonke, J.; Knoery, J. Spatial and temporal distribution of mercury and methylmercury in bivalves from the French coastline. *Mar. Pollut. Bull.* **2017**, *114*, 1096-1102 ; DOI 10.1016/j.marpolbul.2016.10.018.

[185] Remen, M.; Nederlof, M. A. J.; Folkedal, O.; Thorsheim, G.; Sitja-Bobadilla, A.; Pérez-Sánchez, J.; Oppedal, F.; Olsen, R. E. Effect of temperature on the metabolism, behavior and oxygen requirements of *Sparus aurata*. *Aquacult. Environ. Interact*. **2015**, *7*, 115-123 ; DOI 10.3354/aei00141.

[186] Neubauer, P.; Andersen K. H. Thermal performance of fish is explained by an interplay between physiology, behaviour and ecology. *Conserv. Physiol.* **2019**, *7*, coz025. Doi:10.1093/conphys/coz025.

[187] Silva, A.; Carrera, P.; Massé, J.; Uriarte, A.; Santos, M. B.; Oliveira, P. B.; Soares, E.; Porteiro, C. Y.; Stratoudakis, Y. Geographic variability of sardine growth across the northeastern Atlantic and the Mediterranean Sea. *Fish. Res.* **2008**, *90*, 56-69 ; DOI 10.1016/j.fishres.2007.09.011.

[188] Mellon-Duval, C.; de Pontual, H.; Métral, L.; Quemener, L. Growth of European hake (*Merluccius merluccius*) in the Gulf of Lions based on conventional tagging. *ICES J. Mar. Sci.* **2009***, 67,* 62-70 ; DOI 10.1093/icesjms/fsp215.

[189] Lavoie, R. A.; Jardine, T. D.; Chumchal, M. M.; Kidd, K. A.; Campbell, L. M. Biomagnification of mercury in aquatic food webs: a worldwide meta-analysis. *Environ. Sci. Technol*. **2013**, *47*, 13385-13394 ; DOI 10.1021/es403103t.

[190] Borgå, K.; Kidd, K. A.; Muir, D. C. G.; Berglund, O.; Conder, J. M.; Gobas, F. A. P. C.; Kucklick, J.; Malm, O.; Powell, D. E. Trophic magnification factors: considerations of ecology, ecosystems, and study design. *Integr. Envrion Assess. Manag*. **2011**, *8*, 64-84 ; DOI 10.1002/jeam.244.

[191] Alava, J. J.; Cheung W. W. L.; Ross P. S.; Sumaila R. U. Climate change-contaminant interactions in marine food webs: Towards a conceptual framework. *Glob. Change Biol.* **2017***, 23*, 3984-4001 ; DOI 10.1111/gcb.13667.

[192] Du Pontavice, H.; Gascuel, D.; Reygondeau, G.; Maureaud, A.; Cheung W. W. L. 2020, Climate change undermines the global functioning of marine food webs. *Glob. Change Biol.* **2020**, *26*, 1306-1318 ; DOI 10.1111/gcb.14944.

[193] Cresson, P.; Chouvelon, T.; Bustamante, P.; Bãnaru, D.; Baudrier, J.; Le Loc'h, F.; Mauffret, A.; Mialet, B.; Spitz, J.; Wessel, N.; Briand, M.; Denamiel, M.; Doray, M.; Guillou, G.; Jadaud, A.; Lazard, C.; Petit, L.; Prieur, S.; Rouquette, M.; Saraux, C.; Serre, S.; Timmerman, C.A.; Verin, Y.; Harmelin-Vivien, M., 2020. Primary production and depth drive different trophic structure and functioning of fish assemblages in French marine ecosystems. *Progr. Oceanogr.* **2020***, 186*, 102343 ; DOI 10.1016/j.pocean.2020.102343.

[194] Christensen, V.; Walters, C. J. Ecopath with Ecosim: methods, capabilities and limitations. *Ecol. Model*. **2004**, *172*, 109–139 ; DOI 10.1016/j.ecolmodel.2003.09.003.

[195] Christensen, V.; Walters, C. J.; Pauly, D. *Ecopath with Ecosim: A User's Guide*. Fisheries Centre, University of British Columbia, Vancouver, Canada, pp 154; 2005.

[196] Piroddi, C.; Coll, M.; Liquete, C.; Macias, D. M.; Greer, K.; Buszowski, J.; Steenbeek, J.; Danovaro, R.; Christensen, V. Historical changes of the Mediterranean Sea ecosystem: modelling the role and impact of primary productivity and fisheries changes over time. *Sci. Rep.* **2017**, *7*, 44491 ; DOI 10.1038/srep44491

[197] Outridge, P. M.; Macdonald R. W.; Wang F.; Stern G. A.; Dastoor A. P. A mass balance inventory of mercury in the Arctic Ocean. *Environ. Chem.* **2008***, 5*, 89-111 ; DOI 10.1071/EN08002.

[198] *WHO (World Health Organization);* 2017; www.who.int/news-room/fact-sheets/detail/mercury-and-health.

[199] Miklavčič Višnjevec, A.; Kocman, D.; Horvat., M. Human mercury exposure and effects in Europe. *Environ. Toxicol. Chem*. **2013**, *33*, 1259–1270 ; DOI 10.1002/etc.2482.

[200] Basu, N.; Horvat, M.; Evers, D. C.; Zastenskaya, I.; Weihe, P.; Tempowski, J. A State-of-the-Science Review of Mercury Biomarkers in Human Populations Worldwide between 2000 and 2018. *Environ. Health Perpect*. **2019**, *126*, 106001-14 ; DOI 10.1289/EHP3904.

[201] Renzoni, A.; Zino, F.; Franchi, E. Mercury levels along the foodchain and risk for exposed populations. *Environ. Res.* **1997***, 77,* 68–72 ; DOI 10.1006/enrs.1998.3832.

[202] Cammilleri, G.; Vazzana, M.; Arizza, V.; Giunta, F.; Vella, A.; Lo Dico, G.; Giaccone, V.; Giofre, S. V.; Giangrosso, G.; Cicero, N.; Ferrantelli, V. Mercury in fish products: what's the best for consumers between bluefin tuna and yellowfin tuna? *Nat. Prod. Res.* **2018**, *32*(4), 457-462 ; DOI 10.1080/14786419.2017.1309538.

[203] Bellanger, M.; Pichery, C.; Aerts, D.; Berglund, M.; Castaño, A.; Čejchanová, M.; Crettaz, P.; Davidson, F.; Esteban, M.; Fischer, M. E.; Gurzau, A. E.; Halzlova, K.; Katsonouri, A.; Knudsen, L. E.; Kolossa-Gehring, M.; Koppen, G.; Ligocka, D.; Miklavčič, A.; Reis, M. F.; Rudnai, P.; Tratnik, J. S.; Weihe, P.; Budtz-Jørgensen, E.; Grandjean, P.; DEMO/COPHES. Economic benefits of methylmercury exposure control in Europe: Monetary value of neurotoxicity prevention. *Environ. Health* **2013***, 12*, 3. DOI 10.1186/1476-069X-12-3.

[204] Den Hond, E.; Govarts, E.; Willems, H.; Smolders, R.; Casteleyn, L.; Kolossa-Gehring, M.; Schwedler, G.; Seiwert, M.; Fiddicke, U.; Castaño, A.; Esteban, M.; Angerer, J. M.; Koch, H. K. Schindler, B.; Sepai, O.; Exley, K.; Bloemen, L.; Horvat, M.; Knudsen, L. E.; Joas, A.; Joas, R.; Biot, P.; Aerts, D.; Koppen, G.; Andromachi Katsonouri, A.; Hadjipanayis, A.; Krskova, A.; Maly, M.; Mørck, T.A.; Rudnai, P.; Kozepesy, S.; Mulcahy, M.; Mannion, R. C.; Gutleb, A. C. E.; Fischer, M. E.; Ligocka, D.; Jakubowski, M.; Reis, F.; Namorado, S.; Gurzau, A. E., Lupsa,I-R., Halzlova, Michal Jajcaj, M., Mazej, D., Snoj Tratnik, J., López, A.; Lopez, E.; Berglund, M.; Larsson, K.; Lehmann, A.; Crettaz, P.; Schoeters, G. First Steps toward Harmonized Human Biomonitoring in Europe: Demonstration Project to Perform Human Biomonitoring on a European Scale. *Environ. Health Perspect.* **2015***, 123*(3), 255-263 ; DOI 10.1289/ehp.1408616.

[205] Ramon, R.; Murcia, M.; Aguinagalde, X.; Amurrio, A.; Llop, S.; Ibarluzea, J.; Lertxundi, A.; Alvarez-Pedrerol, M.; Casas, M.; Vioque, J.; Sunyer, J.; Tardon, A.; Martinez-Arguelles, B.; Ballester, F. Prenatal mercury exposure in a multicenter cohort study in Spain. *Environ. Int.* **2011***, 37*, 597-604 ; DOI 10.1016/j.envint.2010.12.004.

[206] Mezghani-Chaari, S.; Hamza, A.; Hamza-Chaffai, A. Mercury contamination in human hair and some marine species from Sfax coasts of Tunisia: levels and risk assessment. *Environ. Monit. Assess*. **2011**, *180*, 477–487 ; DOI:10.1007/s10661-010-1800-1.

[207] Miklavčič, A.; Casetta, A.; Snoj Tratnik, J.; Darja Mazej, D.; Krsnik, M., Mariuz, M.; Sofianou, K.; Špirić, Z.; Barbone, F.; Horvat, M. Mercury, arsenic and selenium exposure levels in relation to fish consumption in the Mediterranean area. *Environ. Res.* **2013***, 120*, 7-17 ; DOI 10.1016/j.envres.2012.08.010.

[208] Stratakis, N.; Conti, D. V.; Borras, E.; Sabido, E.; Roumeliotaki, T.; Papadopoulou, E.; Agier, L.; Basagana, X.; Bustamante, M.; Casas, M.; Farzan, S. F.; Fossati, S.; Gonzalez, J. R.; Grazuleviciene, R.; Heude, B.; Maitre, L.; McEachan, R. R. C.; Theologidis, I.; Urquiza, J.; Vafeiadi, M.; West, J.; Wright, J.; McConnell, R.; Brantsaeter, A.-L.; Meltzer, H.-M.; Vrijheid, M.; Chatzi, L. Association of Fish Consumption and Mercury Exposure During Pregnancy with Metabolic Health and Inflammatory Biomarkers in Children. *JAMA Netw Open.* **2020**, *3*(3), e201007 ; DOI:10.1001/jamanetworkopen.2020.1007.

[209] Barbone, F.; Rosolen, V.; Mariuz, M.; Parpinel, M.; Casetta, A.; Sammartano, F.; Ronfani, L.; Vecchi Brumatti L.; Bin, M.; Castriotta, L.; Valent, F.; Little, D. L.; Mazej, D.; Snoj Tratnik, J.; Miklavčič Višnjevec, A.; Sofianou, K.; Špirić, Z.; Krsnik, M.; Osredkar, J.; Neubauer, D.; Kodrič, J.; Stropnik, S.; Prpić, I.; Petrović, O.; Vlašić-Cicvarić, I.; Horvat, M. Prenatal mercury exposure and child neurodevelopment outcomes at 18 months: Results from the Mediterranean PHIME cohort. *Int. J. Hyg. Environ. Health*. **2019**, *222*(1), 9-21 ; DOI 10.1016/j.ijheh.2018.07.011.

[210] Llop, S.; Engström, K.; Ballester, F.; Franforte, E.; Alhamdow, A.; Pisa, F.; Tratnik, J. S.; Mazej, D.; Murcia, M.; Rebagliato, M.; Bustamante, M.; Sunyer, J.; Sofianou-Katsoulis, A.; Prasouli, A.; Antonopoulou, E.; Antoniadou, I.; Nakou, S.; Barbone, F.; Horvat, M.; Broberg, K. Polymorphisms in ABC Transporter Genes and Concentrations of Mercury in Newborns – Evidence from Two Mediterranean Birth Cohorts. *PLoS ONE* **2014**, *9*(5): e97172 ; DOI 10.1371/journal.pone.0097172.

[211] Tranik, J. S.; Falnoga, I.; Trdin, A.; Mazej, D.; Fajon, V.; Miklavčič, A.; Kobal, A. B.; Osredkar, J.; Briški, A. S.; Krsnik, M.; Neubauer, D.; Kodrič, J.; Stropnik, S.; Gosar, D.; Musek, P. L.; Marc, J.; Mlakar, S. J.; Petrović, O.; Vlašić-Cicvarić, I.; Prpić, I.; Milardović, A.; Nišević, J. R.; Vuković, D.; Fišić, E.; Špirić, Z.; Horvat, M. Prenatal mercury exposure, neurodevelopment and apolipoprotein E genetic polymorphism. *Environ. Res*. **2017**, *152,* 375-385 ; DOI 10.1016/j.envres.2016.08.035.

[212] Karagas, M. R.; Choi, A. L.; Oken, E.; Horvat, M.; Schoeny, R.; Kamai, E.; Cowell, W.; Grandjean, P.; Korrick, S. Evidence on the Human Health Effects of Low-Level Methylmercury Exposure. *Environ. Health. Perspect.* **2012***, 120*(6), 799-806 ; DOI:10.1289/ehp.1104494.

[213] Brambilla, G.; Abete, M. C.; Binato, G.; Chiaravalle, E.; Cossu, M.; Dellatte, E.; Miniero, R.; Orletti, R.; Piras, P.; Roncarati, A.; Ubaldi, A.; Chessa, G. Mercury occurrence in Italian seafood from the Mediterranean Sea and possible intake scenarios of the Italian coastal population. *Regul. Toxicol. Pharmacol.* **2013**, *65*, 269-277 ; DOI 10.1016/j.yrtph.2012.12.009.

[214] Amos, H. M.; Jacob, D. J.; Streets, D. G.; Sunderland, E. M. Legacy impacts of all-time anthropogenic emissions on the global mercury cycle. *Global Biogeochem. Cy.* **2013**, *27*, 410–421 ; DOI 10.1002/gbc.20040.

[215]Amos, H. M.; Jacob, D. J.; Kocman, D.; Horowitz, H. M.; Zhang, Y.; Dutkiewicz, S.; Horvat, M.; Corbitt, E. S.; Krabbenhoft, D. P.; Sunderland, E. M. Global biogeochemical implications of mercury discharges from rivers and sediment burial. *Environ. Sci. Technol*. **2014**, *48*, 9514–9522 ; DOI 10.1021/es502134t.

[216] Amos, H. M.; Sonke, J. E.; Obrist, D.; Robins, N.; Hagan, N.; Horowitz, H. M.; Mason, R. P.; Witt; M., Hedgecock, I. M.; Corbitt, E. S.; Sunderland, E. M. Observational and modeling constraints on global anthropogenic enrichment of mercury. *Environ. Sci. Technol*. **2015**, *49*, 4036–4047. Doi.org/10.1021/es5058665.

[217] Schartup, A. T.; Balcom, P. H.; Soerensen, A. L.; Gosnell, K. J.; Calder, R. S. D.; Mason, R. P.; Sunderland, E. M. Freshwater discharges drive high levels of methylmercury in Arctic marine biota. *Proc. Natl. Acad. Sci*. **2015**, *112*, 11789–11794 ; DOI 10.1073/pnas.1505541112.

[218] Soerensen, A. L.; Jacob, D. J.; Schartup, A. T.; Fisher, J. A.; Lehnherr, I.; St. Louis, V. L.; Heimbürger, L.-E.; Sonke, J. E.; Krabbenhoft, D. P.; Sunderland E. M. A mass budget for mercury and methylmercury in the Arctic Ocean. *Global Biogeochem. Cy.* **2016***, 30*, 560–575 ; DOI 10.1002/2015GB005280.

[219] Soerensen, A. L.; Schartup, A. T.; Gustafsson, E.; Gustafsson, B. G.; Undeman, E.; Björn, E. Eutrophication Increases Phytoplankton Methylmercury Concentrations in a Coastal Sea—A Baltic Sea Case Study. *Environ. Sci. Technol*. **2016**, *50*, 11787–11796 ; DOI 10.1021/acs.est.6b02717.

[220] Zhang, Y.; Jaeglé, L.; Thompson, L. A.; Streets, D. G. Six centuries of changing oceanic mercury, *Global Biogeochem. Cy*. **2014**, *28*, 1251–1261, doi:10.1002/2014GB004939.

[221] Zhang, Y.; Jaeglé, L.; Thompson, L. Natural biogeochemical cycle of mercury in a global three-dimensional ocean tracer model. *Global Biogeochem. Cy.* **2014**, *28*(5), 553–570.

[222] Zhang, Y.; Jacob, D. J.; Dutkiewicz, S.; Amos, H. M.; Long, M. S.; Sunderland, E. M. Biogeochemical drivers of the fate of riverine mercury discharged to the global and Arctic oceans, *Global Biogeochem. Cy*. **2015,** *29,* 854–864, doi:10.1002/2015GB005124.

[223] Zhang, Y.; Horowitz, H.; Wang, J.; Xie, Z.; Kuss, J.; Soerensen, A. L. A Coupled Global Atmosphere-Ocean Model for Air-Sea Exchange of Mercury: Insights into Wet Deposition and Atmospheric Redox Chemistry. *Environ. Sci. Technol.* **2019***, 53*, 5052-5061 ; DOI 10.1021/acs.est.8b06205.

[224] Canu, D.; Rosati, G. Long-term scenarios of mercury budgeting and exports for a Mediterranean hot spot (Marano-Grado Lagoon, Adriatic Sea). *Estuar. Coast. Shelf Sci.* **2017**, *198*, 518–528. DOI 10.1016/j.ecss.2016.12.005.

[225] Sunderland, E. M.; Dalziel, J.; Heyes, A.; Branfireun, B. A.; Krabbenhoft, D. P.; Gobas, F. A. P. C. Response of a macrotidal estuary to changes in anthropogenic mercury loading between 1850 and 2000. *Environ. Sci. Technol*. **2010**, *44*, 1698–1704 ; DOI 10.1021/es9032524.

[226] Chen, L.; Zhang, W.; Zhang, Y.; Tong, Y.; Liu, M.; Wang, H.; Xie, H.; Wang, X. Historical and future trends in global source-receptor relationships of mercury. *Sci. Total Environ*. **2018**, *610–611*, 24–31 ; DOI 10.1016/j.scitotenv.2017.07.182.

[227] Sunderland, E. M.; Selin, N. E. Future trends in environmental mercury concentrations: Implications for prevention strategies. *Environ. Health* **2013**, *12*, 2 ; DOI 10.1186/1476-069X-12-2.

[228] Pakhomova, S.; Yakushev, E.; Protsenko, E.; Rigaud, S.; Cossa, D.; Knoery, J.; Couture, R.-M.; Radakovitch, O.; Yabubov, S.; Krzeminska, D.; Newton, A. Modeling the Influence of Eutrophication and Redox Conditions on Mercury Cycling at the Sediment-Water Interface in the Berre Lagoon. *Front. Mar. Sci.* **2018**, *5*, 1-15. DOI 10.3389/fmars.2018.00291.

[229] Rajar, R.; Žagar, D.; Širca, A.; Horvat, M. Three-dimensional modelling of mercury cycling in the Gulf of Trieste. *Sci. Total Environ*. **2000**, *260*, 109–123 ; DOI 10.1016/S0048-9697(00)00555-6.

[230] Ramsak, V.; Malacic, V.; Matjaž, L.; Kotnik, J.; Horvat, M.; Zagar, D. High-resolution pollutant dispersion modelling in contaminated coastal sites. *Environ. Res*. **2013**, *125*, 103–112 ; DOI 10.1016/j.envres.2012.12.013.

[231] Denaro, G.; Salvagio Manta, D.; Borri, A.; Bonsignore, M.; Valenti, D.; Quinci, E.; Cucco, A.; Spagnolo, B.; Sprovieri, M.; and De Gaetano, A.: HR3DHG version 1: modeling the spatiotemporal dynamics of mercury in the Augusta Bay (southern Italy). *Geosci. Model Dev*. **2020**, *13,* 2073–2093 ; DOI 10.5194/gmd-13-2073-2020.

[232] Casas, S.; Bacher; C. Modelling trace metal (Hg and Pb) bioaccumulation in the Mediterranean mussel, *Mytilus galloprovincialis*, applied to environmental monitoring. *J. Sea Res.* **2006**, *56*, 168–181 ; DOI 10.1016/j.seares.2006.03.006.

[233] Kocman, D.; Horvat, M.; Pirrone, N.; Cinnirella, S. Contribution of contaminated sites to the global mercury budget. *Environ. Res*. **2013**, *125*, 160–170 ; DOI 10.1016/j.envres.2012.12.011.

[234] Onrubia, J. A. T.; Petrova, M. V.; Puigcorbé, V.; Black, E. E.; Valk, O.; Dufour, A.; Hamelin, B.; Buesseler, K. O.; Masqué, P.; Le Moigne, F. A. C.; Sonke, J. E.; Rutgers van der Loeff, M.; Heimbürger-Boavida, L.-E. Mercury Export Flux in the Arctic Ocean Estimated from ^{234}Th/^{238}U Disequilibria. *ACS Earth Sp. Chem.* **2020**, *4*(5), 795-801 ; DOI 10.1021/acsearthspacechem.0c00055.

[235] Hammerschmidt, C. R.; Bowman, K. L. Vertical methylmercury distribution in the subtropical North Pacific Ocean. *Mar. Chem*. **2012**, *132–133*, 77–82 ; DOI 10.1016/j.marchem.2012.02.005.

[236] Mason, R. P.; Choi, A. L.; Fitzgerald, W. F.; Hammerschmidt, C. R.; Lamborg, C. H.; Soerensen, A. L.; Sunderland, E. M. Mercury biogeochemical cycling in the ocean and policy implications. *Environ. Res.* **2012***, 119*, 101–117 ; DOI 10.1016/j.envres.2012.03.013.

[237] Lehnherr, I.; St Louis, V. L.; Hintelmann, H.; Kirk, J. L. Methylation of inorganic mercury in polar marine waters. *Nat. Geosci.* **2011***, 4*, 298-302 ; DOI 10.1038/NGEO1134.

[238] Zaferani, S.; Pérez-Rodríguez, M.; Biester, H. Diatom ooze—A large marine mercury sink. *Science* **2018***, 361*, 6404, 797–800. DOI 10.1126/science.aat2735.

[239] Lazzari, P.; Solidoro, C.; Ibello, V.; Salon, S.; Teruzzi, A.; Béranger, K.; Colella, S.; Crise; A. Seasonal and inter-annual variability of plankton chlorophyll and primary production in the Mediterranean Sea: A modelling approach. *Biogeosciences* **2012**, *9*, 217–233 ; DOI 10.5194/bg-9-217-2012.

[240] Cossa, D.; Martin, J. M.; Sanjuan, J. Dimethylmercury formation in the Alboran Sea. *Mar. Poll. Bull.* **1994**, *28*, 381-384.

[241] Wang, K.; Munson, K. M.; Armstrong, D. A.; MacDonald, R. W.; Wang, F. Determining seawater mercury methylation and demethylation rates by the seawater incubation approach: A critique. *Mar. Chem.* **2020***, 219*, 103753 ; DOI 10.1016/j.marchem.2020.103753.

[242] Krabbernhoft, D. P.; Sunderland, E. M. Global Change and Mercury. *Science* **2013**, *341*, 1457-1458 ; DOI 10.1126/science.1242838.

[243] Gittings, J. A.; Raitsos, D. E.; Krokos, G.; Hoteit, I. Impacts of warming on phytoplankton abundance and phenology in a typical tropical marine ecosystem. *Sci. Rep.* **2018**, *8*, 2240 ; DOI:10.1038/s41598-018-20560-5.

[244] Polovina, J. J.; Woodworth, P.A. Declines in phytoplankton cell size in the subtropical oceans estimated from satellite remotely-sensed temperature and chlorophyll, 1998-2007. *Deep-Sea Res. II* **2012**, *77-80*, 82-88 ; DOI 10.1016/j.dsr2.2012.04.006.

[245] Osman, M. B.; Das, S. B.; Trusel, L. D.; Evans, M. J.; Fischer, H.; Grieman, M. M.; Kipfstuhl, S.; McConnell, J. R.; Saltzman, E. S. Industrial-era decline in subarctic Atlantic productivity. *Nature* **2019**, *569*, 551-555 ; DOI 10.1038/s41586-019-1181-8.

[246] Pagès, R.; Baklouti, M.; Barrier, N.; Richon, C.; Dutay, J. C.; Moutin, T. Changes in rivers inputs during the last decades significantly impacted the biogeochemistry of the eastern Mediterranean basin: A modelling study. *Progr. Oceanogr.* **2020**, *181*, 102242. DOI 10.1016/j.pocean.2019.102242

[247] Franz, B. A.; Karaköylül, E. M.; Siegel, D. A.; Westberry, T. K. Global Ocean phytoplankton [in state of the Climate in 2017]. *Bull. American Meteorological Soc*. **2018**, *99*(8), S94-S96.

[248] Gibert, J. P. Temperature directly and indirectly influences food web structure. *Sci. Rep.* **2019**, *9,* 5312. DOI 10.1038/s41598-019-41783-0.

[249] Prinn, R.; Paltsev, S.; Sokolov, A.; Sarofim, M.; Reilly, J.; Jacoby, H. Scenarios with MIT integrated global systems model: significant global warming regardless of different approaches. *Clim. Change* **2011**, *104*, 515–537 ; DOI 10.1007/s10584-009-9792-y.

[250] Giorgi, F.; Gao, X.-J. Regional earth system modeling: review and future directions. *Atmosph. Oceanic Sci. Let.* **2018**, *11,* 189-197 ; DOI 10.1080/16742834.2018.1452520.